FIBERS AS NORMAL AND SPUN-NORMAL SURFACES IN LINK MANIFOLDS

By

BIRCH BRYANT
Bachelor of Science in Mathematics
Southeastern Oklahoma State University
Durant, Oklahoma
2016

Submitted to the Faculty of the
Graduate College of the
Oklahoma State University
in partial fulfillment of
the requirements for
the Degree of
DOCTOR OF PHILOSOPHY
May, 2023

FIBERS AS NORMAL AND SPUN-NORMAL
SURFACES IN LINK
MANIFOLDS

Dissertation Approved:

Dr. Neil Hoffman

Dissertation Advisor

Dr. Henry Segerman

Dr. Jiri Lebl

Dr. Joseph Haley

ACKNOWLEDGMENTS

I would like to thank my advisor Dr. Neil Hoffman for being a wellspring of ideas and resources, and for his tireless editorial aid. This work would have taken me even more years than it has searching for relevant literature that he always seemed to have handy.

I would like to thank Dr. Bus Jaco for his tutelage in my formative years as a mathematician. It is the discussions we had from '18 to '20 that laid the entire groundwork for Chapters 3 and 4. He has fundamentally shaped the way I tackle all problems topological.

I also very grateful for Dr. Charles Matthews for sewing the seed of topology in me; for encouraging me to pursue a graduate degree; and for introducing me to Bus.

I would like to thank my committee for reviewing this thesis and sharing their thoughts and insights.

Finally, I would like to thank my wife, Mingming, and my family for their continued support and patience these six long years. My wife most of all for being an inspirational researcher and the best friend I've ever had.

Acknowledgments reflect the views of the author and are not endorsed by committee members or Oklahoma State University.

Name: BIRCH BRYANT

Date of Degree: MAY, 2023

Title of Study: FIBERS AS NORMAL AND SPUN-NORMAL SURFACES IN LINK MANIFOLDS

Major Field: MATHEMATICS

Abstract: The technique of inflating ideal triangulations developed by Jaco and Rubinstein in [7] gives a procedure starting with an ideal triangulation $\mathcal{T}^*$ of the interior of a compact 3-manifold M, that constructs a triangulation $\mathcal{T}_\Lambda$ of M with real boundary components. This construction is carried out in such a way that combinatorial information from $\mathcal{T}^*$ persists in $\mathcal{T}_\Lambda$. Viewed as an inverse operation, crushing $\mathcal{T}_\Lambda$ along the boundary of M recovers exactly $\mathcal{T}^*$.

We present results from joint work with Jaco and Rubinstein showing, for $\mathcal{T}^*$ and $\mathcal{T}_\Lambda$, there is a bijection between the closed normal surfaces of $\mathcal{T}^*$ and the closed normal surfaces of $\mathcal{T}_\Lambda$. Further corresponding surfaces are homeomorphic. Given the previous relationship for closed normal surfaces, it is natural to inquire about surfaces with boundary. That is, if a surface is normal in $\mathcal{T}_\Lambda$, is there a corresponding spun-normal surface in $\mathcal{T}^*$? In general the answer is no. However, we show that an affirmative answer can be given if the normal surface in $\mathcal{T}_\Lambda$ is in 'C-position.'

In [5], Cooper Tillmann and Worden pose the question *For a fibered knot complement or fibered once-cusped 3-manifold M, is there always some ideal triangulation of M such that the fiber is realized as an embedded spun-normal surface.* We present an algorithm that will construct an inflated triangulation $\mathcal{T}_\Lambda$ in which the fiber is a normal surface in C-position, thus in the underlying ideal triangulation the fiber is realized as a spun-normal surface; answering the question in the affirmative. Further the algorithm will find the spun-normal representation of the fiber.

TABLE OF CONTENTS

LIST OF TABLES

LIST OF FIGURES

CHAPTER I

INTRODUCTION

This thesis studies the combinatorics of properly embedded surfaces in compact 3-manifolds. We view these surfaces through the lens of Normal Surface Theory developed by Kneser [12] in 1929 and expanded upon by Haken [17] in 1961. The theory of normal surfaces was developed to identify incompressible, ∂-incompressible surfaces in a compact 3-manifold. We are then interested in realizing incompressible, ∂-incompressible surfaces with boundary as spun-normal surfaces in ideal triangulations.

In [18] Walsh showed that for a cusped finite volume hyperbolic 3-manifold M with ideal triangulation $\mathcal{T}^*$, any incompressible surface S can be realized as a spun-normal surface in $\mathcal{T}^*$ so long as all edges of $\mathcal{T}^*$ are essential and S is not a virtual fiber. For compact 3-manifolds with boundary which are surface bundles, examples of ideal triangulations with essential edges in which a fiber is not realized as a spun-normal surface are readily constructed. In [5], authors Cooper, Tillmann, and Worden ask the question directly: *For a fibered knot complement or fibered once-cusped 3-manifold M, is there always some ideal triangulation of M such that the fiber is realized as an embedded spun-normal surface?*

As the normalization of surfaces in triangulations with real boundary is well understood, we would like to establish a connection between properly embedded surfaces with boundary in such triangulations, and the spun-normal surfaces in ideal triangulations. In [7], Jaco and Rubinstein develop inflations of ideal triangulations. The process of inflating an ideal triangulation, $\mathcal{T}^*$ of the interior of a 3-manifold M allows one to procedurally build a triangulation $\mathcal{T}_\Lambda$ of M with real boundary that preserves the combinatorics of $\mathcal{T}^*$. By crushing [7] $\mathcal{T}_\Lambda$ along the boundary of M we can fully recover $\mathcal{T}^*$.

We identify three primary purposes for this thesis. First, discussing joint work with Jaco and Rubinstein [2] that establishes the connection between closed normal surfaces in an ideal triangulation $\mathcal{T}^*$ with the closed normal surfaces in $\mathcal{T}_\Lambda$, an inflation of $\mathcal{T}^*$. Secondly, we will show when an analogous connection can be made for normal surfaces with boundary. Lastly, we will use the previous point to give an affirmative answer to the question posed by Cooper, Tillmann, and Worden and an extension to link manifolds. That is, we construct an ideal triangulation of a fibered link manifold in which a fiber is realized as a spun-normal surface. In the case of a knot manifold, we give an algorithm to construct the ideal triangulation and detect the spun-normal fiber.

In Chapter 2, we lay the background. Relevant definitions and results found in the literature appear here. In Section 2.1, we define triangulations, ideal triangulations, and framed triangulations. Triangulations give us the combinatorial framework in which all further work is described. In Section 2.2, we define normal and spun-normal surfaces. As all subsequent sections rely entirely on (spun-)normal surfaces, we have made this section as detailed as possible. In Section 2.3, we give definitions and results surrounding and using efficient triangulations. Our purposes for efficient triangulations is to show we can find desired normal surfaces within a finite collection. In Sections 2.4 and 2.5, we describe the processes of crushing and inflating triangulations. These are the tools with which we build our algorithm in Chapter 4. Section 2.5 contains original procedural methods for constructing frames and for inflating that differ from the source material. The procedure given for inflation has the distinction in that for a given frame, the inflation is uniquely determined, whereas, in [7] there is a choice when inflating a face more than once.

In Chapter 3, we present results coming from work joint with Jaco and Rubinstein completely determining the relationship between closed normal surfaces in ideal triangulations with the closed normal surfaces in inflated triangulations. In particular:

Theorem 3.0.1 (B-Jaco-Rubinstein) *Let M be a compact 3-manifold with nonempty boundary no component of which is a 2-sphere. Suppose $(\mathcal{T}^*, \Lambda)$ is a framed triangulation*

of $\mathring{M}$, and $\mathcal{T}_\xi$ is the inflation of $\mathcal{T}^*$ for some frame $\xi \in \Lambda$. The combinatorial crushing map determined by crushing $\mathcal{T}_\xi$ along ∂M induces a bijection between the closed normal surfaces in $\mathcal{T}_\xi$ and the closed normal surfaces in $\mathcal{T}^*$; furthermore, corresponding surfaces are homeomorphic.

We end the chapter with a result about efficiency of inflated triangulations. It is the work found here that inspired the results of Chapter 4.

In Chapter 4, we work towards answering the question stated in the abstract of Cooper, Tillmann, and Worden. In Section 4.1, we discuss the effects of Pachner moves on inflated triangulations. In Section 4.2, we give a sufficient condition for a normal surface in an inflation triangulation to determine a spun-normal surface in the corresponding ideal triangulation. This correspondence is not a bijection as with results from Chapter 3. We finish Section 4.3 with the main theorems:

Theorem 4.3.2 *Let K be a compact, irreducible, ∂-irreducible, atoroidal 3-manifold with nonempty connected boundary a torus. Further suppose that K is an orientable S^1 bundle over an essential fiber F. There is an algorithm to build an ideal triangulation of the interior K in which F spun-normalizes. The algorithm finds the spun-normal surface.*

This answers Cooper, Tillmann, and Worden in the affirmative. We then have the most generalized result of our work, constructing an ideal triangulation for a link manifold that is a surface bundle in which a fiber of the bundle structure is realized as a spun-normal surface. This gives a partial answer to a question of Walsh [18].

Theorem 4.3.4 *Let L be a compact, irreducible, ∂-irreducible, atoroidal 3-manifold with nonempty boundary, each component of which is a torus. Further, suppose that L is an orientable S^1-bundle over an essential fiber F. There is an algorithm to build an ideal triangulation of the interior of L in which F spun-normalizes. The algorithm finds the spun-normal surface.*

CHAPTER II

BACKGROUND

2.1 Triangulations

An n-manifold (with boundary), M, is defined as any Hausdorff space with a countable basis in which every point has an open neighborhood homeomorphic to open ball (or half-ball) in $\mathbb{R}^n$ (or H^n the upper half space of $\mathbb{R}^n$). We restrict M to be compact and to have nonempty boundary, no component of which is a 2-sphere.

Let $\mathbf{\Delta}$ be a finite collection of pairwise disjoint oriented tetrahedra, $\tilde{\Delta}_i$ together with a collection Φ of homeomorphisms (orientation reversing) from one 2-cell, $\tilde{\sigma}_j$, of $\tilde{\Delta}_i$ to a 2-cell, $\tilde{\sigma}_m$, of some $\tilde{\Delta}_k$ (possibly $i = k$). We give $\mathbf{\Delta}$ the weak topology induced by Φ. If $X = \mathbf{\Delta}/\Phi$ is homeomorphic to a 3-manifold M, we denote the collection of tetrahedra together with the face pairings as $\mathcal{T}$ and say that $\mathcal{T}$ is a triangulation of M. If at each vertex, v_i, X is not a manifold point we say that v_i is an *ideal vertex* and classify v_i by the boundary of its regular neighborhood. In this case $X \backslash \{vertices\}$ is the interior of a compact 3-manifold with boundary, M. We denote the collection of tetrahedra and the face pairings as $\mathcal{T}^*$ and say that $\mathcal{T}^*$ is an *ideal triangulation* of the interior of M. We denote the image of $\tilde{\Delta}_i$ as Δ_i and call $\tilde{\Delta}_i$ the *lift* of Δ_i.

The above notation will be used throughout the paper to refer to non-specific n-cells of the tetrahedra. In order to facilitate the reader in following and working examples for themselves, we translate to the notation of REGINA[4]. In this regard tetrahedra are simply referred to by a number $\Delta_i \to i$, faces denoted $(i)(abc)$ where i represents the tetrahedron and $a, b, c \in \{0, 1, 2, 3\}$ refers to the vertices present; edges $(i)(ab)$, a, b again referring to the

vertices. It is sometimes convenient when the tetrahedron index is understood to drop the preceding (i), thus we see edge (03) in tetrahedron 5 say. Likewise if the tetrahedron has a specific name say, $\Delta_i = \mathcal{P}$, we may denote a face as $(\mathcal{P})(012)$.

More generally we can construct cellulations. Beginning with a set of discrete points, X^0 we inductively create X^n by attaching n-balls, e_i^n, via boundary homeomorphisms $\phi_i : S^{n-1} \to X^{n-1}$. As with triangulations above X^n is given the weak topology relative to the collection of all maps ϕ_i and if $M \sim X^n$ then we say that X^n is a *cell structure* of M. Each X^i is the **i-skeleton** of X^n. We are particularly interested in cell structures on 2-manifolds composed of triangles and quadrilaterals.

A *spine*, ξ, of a triangulated surface, S, is a graph in the 1-skeleton such that each component of its complement in S is a disc. We say that ξ is a *frame* if the complement in S is a single disc. A vertex of ξ is called a *branch point* if it has index larger than 2. A maximal path in ξ containing no interior vertices a branchpoint is called a *branch*.

For a triangulation with an ideal vertex v, the intersection of the boundary of a small regular neighborhood, S of v with the tetrahedra of $\mathcal{T}^*$ gives a triangulation of S (discussed further in Section 2.2). Each vertex of S then corresponds to one end of an edge in $\mathcal{T}^*$, and an edge, e, meets the collection of vertex-linking surfaces in two points. We denote these two points as e^+ and e^-. By our naming convention we have determined an orientation on e, directed from e^- to e^+. Suppose that D_e^+ and D_e^- are small regular neighborhoods of e^+ and e^- respectively, in the vertex-linking surfaces. The triangulation of the vertex-links induce a cellulation of D_e^+, D_e^-. If σ is a face in $\mathcal{T}^*$ having e as an edge, there are unique edges, one in D_e^+ and one in D_e^-, lying in σ, meeting e. We say that one edge is *above* the other relative to the orientation on e. Let $x_i, x_{i+1}, y_j, y_{j+1}$ be edges in the frame ξ, with $x_i, x_{i+1} \subset D_e^+$ and $y_j, y_{j+1} \subset D_e^-$. Denote by $\tilde{y}_j, \tilde{y}_{j+1}$ the edges above y_j, y_{j+1} in D_e^+. If the path in D_e^+ formed by the edges x_i, x_{i+1} crosses the path formed by $\tilde{y}_j, \tilde{y}_{j+1}$ (illustrated in Figure 1) we say that ξ has a *crossing* at e.

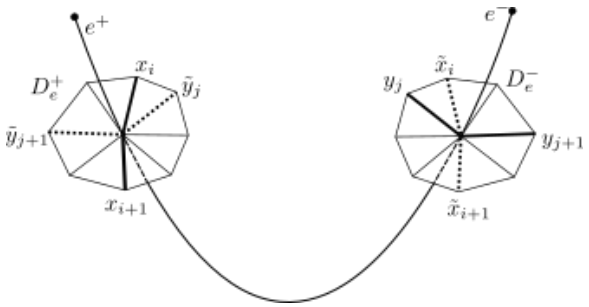

Figure 1: A crossing of x_i, x_{i+1} and $\tilde{y}_j, \tilde{y}_{j+1}$.

Definition 2.1.1 *Let ξ be a frame for a triangulated surface S. Let ϵ be the number of edges in ξ and c be the number of crossings. Define the* ***length*** *by $len(\xi) = e + 2c$; similarly the* ***complexity*** *is defined by $\mathcal{C}(\xi) = e + c + 4g - 2$, where g is the genus of S.*

Let $\Lambda = \{\xi_i\}$ be a collection of frames. We extend the notions of length and complexity to the collection Λ:

$$len(\Lambda) = \sum_i len(\xi)$$

$$\mathcal{C}(\Lambda) = \sum_i \mathcal{C}(\xi)$$

Definition 2.1.2 *A* ***framed triangulation*** *$(\mathcal{T}^*, \Lambda)$ consists of a triangulation with ideal vertices and a collection of $\Lambda = \{\xi_i\}$ of frames such that for each ideal vertex v_i of $\mathcal{T}^*$ we have a corresponding frame ξ_i.*

For a framed triangulation $(\mathcal{T}^*, \Lambda)$ for which all vertices are ideal, $\mathcal{T}^*$ agrees with the usual definition of an ideal triangulation. We say that $(\mathcal{T}^*, \Lambda)$ is a framed triangulation for a compact 3-manifold with boundary M if the interior of the topological space given by $\mathcal{T}^*$ is homeomorphic to the interior of M. We will restrict to the case where $\mathcal{T}^*$ is a minimal vertex triangulation. This implies that each vertex, either ideal or real, corresponds to a boundary component of M.

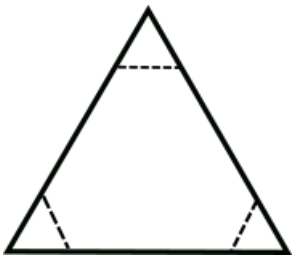

Figure 2: The three normal arc types.

2.2 Normal surfaces

Normal surface theory has been used to great effect in algorithmic analysis of 3-manifolds. Though treated slightly different than in the modern theory, Haken [17] used normal surfaces to algorithmically detect the unknot. Recently, joint with Jaco and Rubinstein [2], we used the theory to simplify the combinatorial structure of triangulated 3-manifolds so that it better captures the geometry of said manifold.

What follows is a brief review of the theory of normal surfaces. It is foundational to the works of this thesis, thus we will attempt to be robust.

Definition 2.2.1 *If $\tilde{\Delta}$ is a compact, convex, linear cell and $\tilde{\sigma}$ is a face of $\tilde{\Delta}$, an arc in $\tilde{\sigma}$ is a **normal arc** if its endpoints lie in the interior of separate edges of $\tilde{\sigma}$.*

For the triangular faces of a 3-manifold triangulation, we have three distinct normal arcs illustrated in Figure 2. Normal arcs, though in one dimension lower, are paramount in this theory. The connection is illustrated in the following definition.

Definition 2.2.2 *Let $\tilde{\Delta}$ be a compact, convex linear cell. A **normal disc**, D in $\tilde{\Delta}$ is a properly embedded disc whose interior lies in the interior of $\tilde{\Delta}$ and whose boundary consists of normal arcs in faces $\tilde{\sigma}$ of $\tilde{\Delta}$, no face having more than one normal arc type belonging to D.*

A *normal isotopy* is an isotopy invariant on each simplex of $\tilde{\Delta}$. The normal isotopy class of a normal disc is the *disc type*. For a tetrahedron $\tilde{\Delta}_i$ in the triangulation $\mathcal{T}$ of 3-manifold

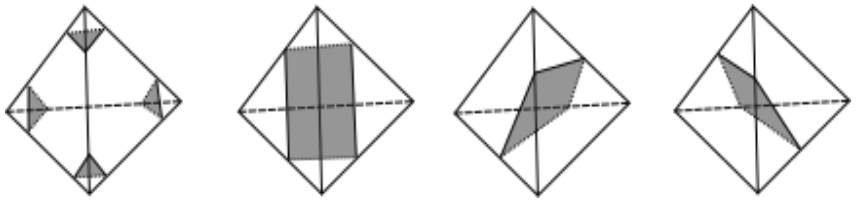

Figure 3: Four normal triangle and three normal quad types.

M, we thus have seven distinct normal discs types, three normal quadrilateral types and four normal triangular types as illustrated in Figure 3.

Definition 2.2.3 *Let M be a compact 3-manifold with triangulation $\mathcal{T}$. Let S be a properly embedded surface in M transverse to the 2-skeleton of $\mathcal{T}$. Suppose that Δ_i is a tetrahedron of $\mathcal{T}$ and let c be a cell of S induced by $\mathcal{T}$. Then c is the image of the lift $\tilde{c}$ in $\tilde{\Delta}_i$. If all such cells c constructed this way are normal discs, then S is a* ***normal surface*** *relative to $\mathcal{T}$.*

We extend the above definition to framed triangulations and as a result to ideal triangulations.

Definition 2.2.4 *Let M be a compact 3-manifold with framed triangulation $(\mathcal{T}^*, \Lambda)$. Let S be an embedded surface in M transverse to the 2-skeleton of $\mathcal{T}^*$. Suppose that Δ_i is a tetrahedron of $\mathcal{T}^*$ and let c be a cell of S induced by $\mathcal{T}^*$. Then c is the image of the lift $\tilde{c}$ in $\tilde{\Delta}_i$. If all such cells c constructed this way are normal discs, and*

1. *the number of such normal discs is finite, then S is a again a* ***normal surface*** *relative to $\mathcal{T}^*$.*

2. *the number of normal quadrilaterals is finite and the number of normal triangles is infinite, then S is a* ***spun-normal surface*** *relative to $\mathcal{T}^*$.*

The collection of infinitely many normal triangles in the above definition forms infinitely long annuli, A_i spinning toward the ideal boundary components B_i. Here 'infinitely long' refers the homeomorphism $A_i \cong S^1 \times [0, \infty)$. For a subcomplex S_T of the spun-normal surface S we say that S_T is a *tail* if its interior is connected and the interior of the complement

$S_C = S \backslash S_T$ is homeomorphic to the interior of S. We say that S_C is a *core* of S. Note this definition of core is more general than commonly found in the literature [10].

Definition 2.2.5 *Given a normal arc γ in a face $\tilde{\sigma}$, γ is isotopic to the boundary of a regular neighborhood of the lift of some vertex v in $\tilde{\sigma}$. We say that γ **links** the vertex v. Similarly given a normal triangle, c, in a tetrahedron $\tilde{\Delta}_i$, c is isotopic to the boundary of a regular neighborhood of the lift of some distinct vertex v in $\tilde{\Delta}_i$. We say that c **links** the vertex v.*

At times we will alternate in saying that a normal surface S is normal in M and normal in $\mathcal{T}$ to emphasize one construct over the other. Now that we have defined normal surfaces it is natural to ask if any exist for an arbitrary triangulation.

Definition 2.2.6 *The collection of all normal triangles linking a distinct vertex v, is called a **vertex-linking surface**, S_v.*

We then have a first statement about the existence of a normal surface:

Proposition 2.2.1 *Let M be a compact 3-manifold with framed triangulation $(\mathcal{T}^*, \Lambda)$. Let v be a vertex in $\mathcal{T}^*$. The vertex-linking surface S_v is a normal surface in $\mathcal{T}$.*

The following definition can be found in [2] and will be used extensively from Section 2.4 onwards.

Definition 2.2.7 (B-Jaco-Rubinstein) *Let M be a 3-manifold with nonempty boundary, $\mathcal{T}$ a triangulation (or $(\mathcal{T}^*, \Lambda)$ a framed triangulation) with real boundary component B. That is $\mathcal{T}$ ($\mathcal{T}^*$) has unglued faces of tetrahedra given a triangulation of B. If the boundary of a small regular neighborhood of B is normally isotopic to a normal surface, then we say that M has normal boundary at B and we call this surface the **boundary-linking surface**.*

It is not necessary in general that a boundary-linking surface exists for all components ∂M. For example a 0-efficient (see Section 2.3) triangulation of a 3-cell has no normal 2-spheres and thus no normal boundary [2]. A second example can be found in minimal

layered-triangulations of solid tori. The boundary torus is not normal as a minimal layered-triangulation of a solid torus has no normal tori [9].

We also have classic existence theorems dating back to the foundational works of Kneser and Haken [12, 17].

Theorem 2.2.1 (Kneser) *Let M be a 3-manifold. If M has an essential, properly embedded disc, then for any triangulation $\mathcal{T}$ of M there is a properly embedded essential normal disc in $\mathcal{T}$.*

Theorem 2.2.2 (Kneser) *Let M be a 3-manifold. If M has an essential, properly embedded 2-sphere, then for any triangulation $\mathcal{T}$ of M there is an essential, properly embedded normal 2-sphere in $\mathcal{T}$.*

Given an embedding of a surface S in a 3-manifold M it is natural to ask, "What if the given embedding is not normal?" What can be done with S (or $\mathcal{T}$) to obtain a normal surface? We say that S is *realized* as a (spun-)normal surface if S is isotopic (not necessarily normal isotopic) to a normal surface. We call this normal surface a *normal representative* of S and when no confusion would arise, simply denote the normal representative by S. We must point out that a normal representative is not necessarily unique. An example of non-uniqueness can be seen in the proof of Proposition 3.0.1. To reflect the language used commonly in the literature, we simply say that S *(spun-)normalizes* if S is realized as a (spun-)normal surface.

Theorem 2.2.3 (Haken) *Let M be a 3-manifold with triangulation $\mathcal{T}$ (with no ideal vertices), S an incompressible, ∂-incompressible properly embedded surface in M transverse to the 2-skeleton of $\mathcal{T}$. Then S normalizes in $\mathcal{T}$.*

So by Theorem 2.2.3 an incompressible, ∂-incompressible properly embedded surface, S shrinks to a normal surface that is homeomorphic to S. We can thus expect to find many normal surfaces in a given triangulation. It would therefore be expedient to be able to parameterize all normal surfaces.

If $\mathcal{T}$ is a triangulation, there are $7n$ distinct normal disc types in $\mathcal{T}$ where $n = |\mathcal{T}|$ is the number of tetrahedra in $\mathcal{T}$. Then a normal surface in S can be a assigned a vector $v \in \mathbb{R}^{7n}$.

Definition 2.2.8 *Let M be a 3-manifold with triangulation (or ideal triangulation) $\mathcal{T}$, with $n = |\mathcal{T}|$. Let S be a normal surface in $\mathcal{T}$. We parameterize S with the* ***vector representation*** *$\vec{S} \in \mathbb{Z}^{7n}_{\geq 0}$ with vector coordinates:*

$$\vec{S} = (x_{00}, x_{01}, x_{02}, x_{03}, y_{01}, y_{02}, y_{03}, ..., x_{n0}, x_{n1}, x_{n2}, x_{n3}, y_{n1}, y_{n2}, y_{n3}) \in \mathbb{Z}^{7n}_{\geq 0} \tag{2.2.1}$$

where the entry x_{ij} corresponds to the number of normal triangles in tetrahedra i of type t_{ij} linking the lift of the vertex j. The entry y_{ij} corresponds to the number of normal quadrilaterals in tetrahedron i of type q_{ij} linking the edge $(0j)$.

The vector representation $\vec{S}$ for a normal surface S is further constrained by a system of linear equations. Given a normal arc type γ in the 2-skeleton, γ lifts to two distinct normal arc types $\tilde{\gamma}$ and $\tilde{\gamma}'$ in tetrahedra $\tilde{\Delta}_i, \tilde{\Delta}_j$ (possibly $i = j$). In each respective tetrahedron there are exactly two normal disc types (a triangle and a quadrilateral) whose boundaries contain normal arcs of the respective type. Let these types correspond to the disc types $t_{ir}, q_{is}, t_{jr'}, qjs'$. Then the number of normal arcs of type $\tilde{\gamma}$ must be given by $x_{ir} + y_{is}$, likewise the number of normal arcs of type $\tilde{\gamma}'$ is given by $x_{jr'} + y_{js'}$. Thus if the normal surface S intersects the 2-skeleton with normal arc type γ, we have the linear equation

$$x_{n_i} + y_{m_i} = x_{n_j} + y_{m_j} \tag{2.2.2}$$

Equation 2.2.2 is a so called **matching equation**. Thus v is a solution to a system of $6n - 3b/2$ linear equations (three for each face gluing in $\mathcal{T}$) where b is the number of unglued faces. We have an even stronger relation between the normal surfaces and the matching equations [17]:

Theorem 2.2.4 *Let $\mathcal{T}$ be a triangulation with t tetrahedra. Let v be a vector in the positive orthant of $\mathbb{R}^{7t}$ with coordinates corresponding to normal disc types as in Definition 2.1.6.*

There is a normal surface S (possibly disconnected) in $\mathcal{T}$ with vector representation v if and only if v satisfies the system of linear equations described by Equation 2.1.1. Further S is embedded if and only if for each triplet at most one of y_{i0}, y_{i1}, y_{i2} is nonzero.

In the case that at most one of y_{i0}, y_{i1}, y_{i2} is nonzero, we say that $\vec{S}$ is *admissible* and this constraint is referred to as the *Quadrilateral Condition*. We will prove only the latter claim.

Proof. Examining normal quadrilaterals in a tetrahedron $\tilde{\Delta}_i$, we see that if two or more types are present that they will have nonempty intersection. Thus S was not embedded. If on the contrary, only one of y_{i0}, y_{i1}, y_{i2} is nonzero, then the normal discs represented by the coordinates $x_{i0}, x_{i1}, x_{i2}, x_{i3}, y_{i0}, y_{i1}, y_{i2}$, can be arranged in $\tilde{\Delta}_i$ so as to have empty intersection. Hence, we have an embedding on the interior of $\tilde{\Delta}_i$. Combining this embedding with the embedding induced on the 2-skeleton and 1-skeleton by the matching equations, we conclude that S is embedded. ■

Thus the appropriate parameterization of normal surfaces in $\mathcal{T}$ is by the following:

Definition 2.2.9 *Normal surfaces S with vector representations $\vec{S}$ are non-negative integral solutions to the system of linear equations described in Equation 2.2.2 thus we obtain a convex cone in $\mathbb{R}^{7t}$ consisting of all vector representations v called the **solution cone** $\mathcal{S}(M, \mathcal{T})$.*

Definition 2.2.10 *If in addition to the constraints defining $\mathcal{S}(M, \mathcal{T})$, we require $\sum_i t_i + \sum_j q_j = 1$ then we obtain a compact convex linear cell, the rational points of which represent projective classes of normal surfaces. We denote this compact convex linear cell, $\mathcal{P}(M, \mathcal{T})$, the **projective solution space** of $\mathcal{S}(M, \mathcal{T})$. We denote the projective class of S by $\bar{S}$.*

Definition 2.2.11 *The **carrier** of a normal surface S is the unique minimal face of $\mathcal{P}(M, \mathcal{T})$ containing $\bar{S}$.*

With this parameterization we can define a binary relation on the set of normal surfaces as follows:

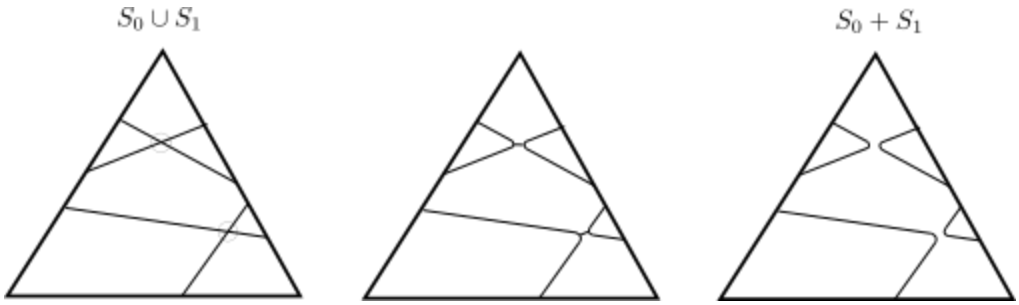

Figure 4: Exchange at normal arcs in the 2-skeleton.

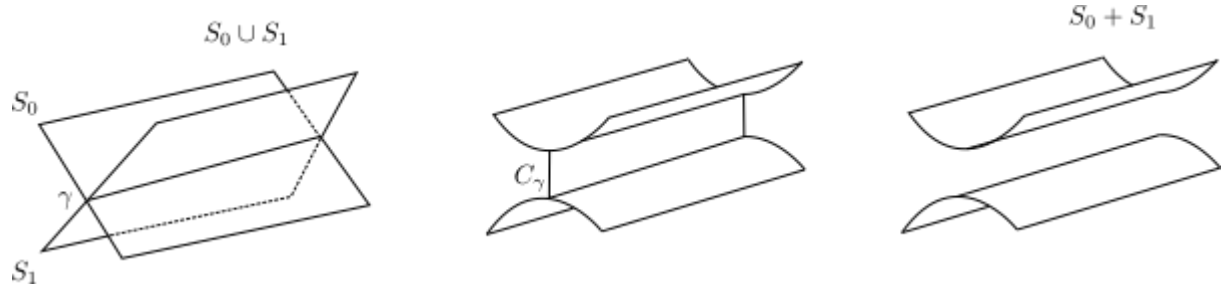

Figure 5: Exchange along the *exchange band* C_γ.

Definition 2.2.12 *Given normal surfaces S_0, S_1 with respective vector representations $\vec{S_0}, \vec{S_1}$, we define the* ***normal sum*** *$S_0 + S_1 = S$ to be the resulting normal surface (likely not embedded) given by the vector representation of the vector sum $\vec{S_0} + \vec{S_1} = \vec{S}$. If S is properly embedded, then we say that S_0 and S_1 are* ***compatible****.*

We call $S = S_0 + S_1$ a *Haken decomposition* of S. It is of course possible for S to have numerous distinct Haken decompositions. There is a geometric interpretation of the normal sum given by a cutting argument along the arcs and curves in $S_0 \cap S_1$. The cutting is completely determined by the intersection of normal arcs in the 2-skeleton of $\mathcal{T}$. This operation is an *exchange* illustrated in Figures 4 and 5. The band $C_\gamma = \gamma \times [0, 1]$ in Figure 5, is called the *exchange band*; the normal sum $S_0 + S_1$ is obtained by cutting each exchange band C_γ for all components γ of $S_0 \cap S_1$.

Definition 2.2.13 *A normal surface S is a* ***fundamental surface*** *if it cannot be written as a sum $S = S_0 + S_1$ for any nonempty S_0, S_1. S is said to be a* ***vertex surface*** *if kS cannot be written $kS = nS_0 + mS_1$ for any non-negative integers k, n, m and nonempty*

surfaces S_0, S_1 that are not normal isotopic to S.

An equivalent definition for a vertex solution is a surface S such that the projective class $\bar{S}$ lies at a vertex of $\mathcal{P}(M, \mathcal{T})$. Fundamental and vertex solutions have been seminal in normal surface theory. It is often the case (as it will be later in this work) that when searching for a normal representative for a given surface, that we need look no further than these special solutions. In a worse (yet not catastrophic) case one is likely to be able to construct the desired surface from vertex solutions, hopefully in some linear (or bounded) number of steps.

In Chapter 4, we will find obstructions to spun-normalization in the form of normal quadrilaterals. One then wonders, are the normal triangles necessary in identifying these obstructing normal quadrilaterals? In [16], Tollefson showed the normal quadrilateral types are sufficient to identify all normal and spun-normal surfaces. We will summarize these results here. From 2.2.1 we take the y_{ij} entries to form the *normal Q-coordinates* of S

$$\vec{S}_Q = (y_{01}, y_{02}, y_{03}, ...y_{n1}, y_{n2}, y_{n3}) \in \mathbb{Z}^{3n}_{\geq 0}.$$

Like the normal coordinates in Equation 2.2.1 the normal Q-coordinates are a solution to a linear system of equations. Consider an edge $e_k = (ab)$ in a tetrahedron t with positive orientation from a to b and assume a right hand twist around e. There are exactly two normal quadrilateral types incident to e, call them q_i, q_j (q_l being non-incident to e_k). Each disc of type q_i and q_j has within its boundary, a normal arc linking vertex a in a face of t containing e and a normal arc linking vertex b in the other face containing e_k. If for the disc type q_i a right handed twist around e_k moves from the face containing the normal arc of q_i linking b to the face containing the normal arc linking a, we define the *sense* of q_i to be $\epsilon_{k,i} = +1$. For the disc type q_j, q_l we set $\epsilon_{k,j} = -1, \epsilon_{k,l} = 0$ (illustrated in Figure 6).

Consider for a normal surface S, all normal quadrilateral types incident to some edge e_k in triangulation $\mathcal{T}$. The number of normal quadrilateral types of positive sense must be equal to the number of negative sense. Thus the vector $\vec{S}_Q$ is a solution to the linear system of equations, the *Q-matching equations*:

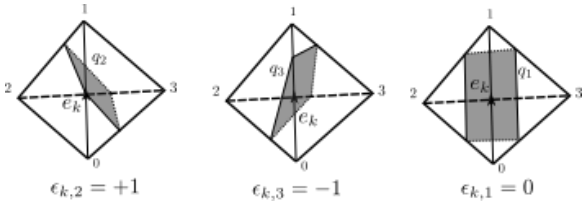

Figure 6: The sense of each q_i respective to the edge e_k.

$$\left\{ \sum_{i=1}^{3n} \epsilon_{k,i} y_i = 0 \right\}_k \tag{2.2.3}$$

We then have form [16]:

Theorem 2.2.5 (Tollefson) *Let M be a compact 3-manifold with a fixed (ideal)triangulation. If S is a (spun-)normal surface in M then the Q-coordinates $\vec{S}_Q$ give an admissible solution to the Q-matching equations. Moreover if $\vec{v}$ is a nonzero admissible solution to the Q-matching, equations then there is a unique (spun-)normal surface S in M with no trivial components such that $\vec{S}_Q = \vec{v}$.*

All notions of the solution space, fundamental and vertex solutions derived from the matching equations carry over to the Q-matching equations. Likewise a Haken sum translates to vector addition in normal Q-coordinates.

2.3 Efficient Triangulations

If M is an orientable 3-manifold and $\mathcal{T}^*$ is a (framed) triangulation of M, we say that $\mathcal{T}^*$ is *0-efficient* if the only normal 2-spheres are vertex-linking and the only normal discs (i.e. a 2-cell) are vertex-linking. For an orientable triangulation, $\mathcal{T}$, (with no ideal vertices) $\mathcal{T}$ is 0-efficient and the only normal tori are boundary-linking, we say that $\mathcal{T}$ is *1-efficient*. Similarly, for a 0-efficient framed triangulation $(\mathcal{T}^*, \Lambda)$ if the only normal tori are either vertex-linking or boundary-linking, then $\mathcal{T}^*$ is again said to be *1-efficient*.

Efficiencies are combinatorial restrictions on (ideal-)triangulations that allow one to make statements about what essential surfaces can be properly embedded in the associated man-

ifold. The usual method as we see later in this section, is to use efficiency to argue that an essential surface can be found amongst the fundamental surfaces of the triangulation [8, 14]. A closely related notion to efficiency, is that of angle structures. Angle structures are in contrast a geometric restriction on ideal triangulations. Angle structures allow one to associate the ideal tetrahedra with ideal hyperbolic simplices. We will focus on a generalization of angle structures and use the definition described in [10]. Lackenby uses an equivalent definition in [13], but the following defintion by Kang and Rubinstein from [10] is more applicable here.

Definition 2.3.1 (Kang-Rubinstein) *Given an ideal triangulation $\mathcal{T}^*$ of the interior of a 3-manifold M, a **taut angle structure** is an assignment of angles 0 or π to the dihedral angles between faces in each tetrahedron of $\mathcal{T}^*$ satisfying the following criteria:*

1. *For each tetrahedron Δ there are four angles of measure 0 and two of measure π. The two π angles are assigned to opposite edges of Δ.*

2. *For every edge e of $\mathcal{T}^*$, the sum of all angles at e is 2π.*

If $\mathcal{T}^*$ admits a taut angle structure then we say that $\mathcal{T}^*$ is a taut ideal triangulation. We specifically choose to use taut angle structures in this work for the application of the following theorem that follows from work by Lackenby [13]:

Theorem 2.3.1 (Lackenby) *Let M be a compact, orientable, irreducible, ∂-irreducible, atoroidal, annanular 3-manifold with boundary. There is an algorithm to construct a taut ideal triangulation of $\mathring{M}$.*

The connection between taut angle structures and efficiency can be seen in the following weaker version of Theorem 2.6 of [10]:

Proposition 2.3.1 *Let M be an atoroidal 3-manifold with nonempty boundary and $\mathcal{T}^*$ an ideal triangulation of $\mathring{M}$. If $\mathcal{T}^*$ admits a taut angle structure then $\mathcal{T}^*$ is 1-efficient.*

Our use of efficiency, in particular 0-efficiency will be to find normalizations of fibers of surface bundles. Let us first define surface bundles and then discuss how to find the desired normalizations.

Definition 2.3.2 *Let F be a compact orientable surface and let $h : F \to F$ be a homeomorphism. The* ***mapping torus*** *h is the space $F \times I/\sim$ with the given equivalence relation $(x, 1) \sim (h(x), 0)$.*

Definition 2.3.3 *Let M be a 3-manifold. A* ***surface bundle structure*** *on M is a pair (h, ϕ) where h is a homeomorphism of F and ϕ is a homeomorphism between the mapping torus of h and M.*

The following Theorem 2.3.2 from [14] needs a great deal of machinery to prove. As we will not need the machinery for the main results of this work we shall omit most of the proofs referring again to [14]. The problem however is the that theorem applies to closed 3-manifolds and we would like to make an analogous statement about manifolds with torus boundary. We will present the required lemmas and the proof of Theorem 2.3.2 translated from how they appear in [14] with only additional background definitions presented. While the lemmas are due to Thompson, the versions stated in [14] are more relevant for this work.

We turn our attention to the intersections of normal surfaces.

Definition 2.3.4 (Schleimer) *Suppose that H is a normal surface in $\mathcal{T}$, $H = F + G$ a Haken decomposition of H. We say that H is* ***neat*** *if F and G*

1. *intersect transversely,*
2. *$F \cap G$ intersects the 2-skeleton of $\mathcal{T}$ transversely, and*
3. *G minimizes the lexicographic complexity*

$$(|F \cap G'|, |(F \cap G') \backslash \mathcal{T}^2|)$$

among all G' normally isotopic to G such that F and G' satisfy the first two conditions.

Definition 2.3.5 (Schleimer) *Given an annulus A properly embedded in a 3-manifold M, we say that A is a **tent** if ∂A bounds an annulus B in ∂M, $A \cup B$ bounds a "cube with a knotted hole" inside of M and a component of the boundary of A, $\partial_+ A$ bounds a disc in ∂M.*

Recall the definition of exchange bands from Section 2.2. Exchange bands must be either discs, annuli or Mobius bands. Exchange annuli being tents is bothersome. There may be elements of $\pi_1((M \backslash H) \backslash A)$ that are not in $\pi_1(M \backslash H)$.

Lemma 2.3.1 (Thompson) *Suppose that*

1. *M is an orientable 3-manifold not homeomorphic to S^3 with 0-efficient triangulation $\mathcal{T}$,*
2. *Let H be a normal surface or almost normal surface with exceptional piece a single octagon, and*
3. *H is two sided.*

Then no neat Haken decompositon of H admits an excange annulus which is a tent in $M \backslash H$.

Lemma 2.3.2 (Thompson) *Suppose that*

1. *M is an orientable 3-manifold with connected boundary component a torus with 0-efficient triangulation $\mathcal{T}$,*
2. *H is a closed, connected, two-sided surface embedded in M which is not a 2-sphere or a disc,*
3. *H is normal or almost normal, and*
4. *$H = F + G$ is a neat Haken decomposition with all exchange annuli trivial*

It follows that there is a Haken decomposition $H = H' + G'$ of H where G' is nonempty and H' is isotopic to H.

Proof. For an exchange annulus A (that is, we have a curve of intersection in $F \cap G$ away from ∂M) the proof of Lemma 2.3.2 follows exactly that of Lemma 5.1.8 in. [14]. For an exchange disc A, the proof follows analogously to the case when the exchange annulus is a tube. ■

We again stress the following corollary and proof are as found in [14] with theorem and lemma references pointing to the respective statements found herein.

Corollary 2.3.1 (Schleimer) *All acylidrical surfaces in M are isotopic to fundamental normal surfaces.*

An embedded surface, H in M is *acylindrical* if H is two-sided, incompressible and $M \backslash H$ admits no essential annuli.

Proof. Fix an acylindrical surface H. By Thoerem 2.2.3 isotope H to be normal. Pick a least weight such normal surface, which we will again call H. Suppose that this surface is not fundamental.

Let $H = F + G$ be a neat Haken decomposition for H. Note that, as H is acylindrical, all exchange bands must be trivial. If there is an exchange band which is a Mobius strip, then H is either the boudnary of a solid torus or M is homeomorphic to $\mathbb{RP}^3$, both contradictions.

It follows that all exchange bands are annuli. By Lemma 2.3.1 none of these are tents. If there are any tubes or tunnels then by Lemma 2.3.2 there is a surface H' isotopic to H of lesser weight. But this a contradiction. We conclude that there are no exchange annuli at all, i.e. H is fundamental. ■

Finally we have the theorem to be used in Chapter 4 following from the above results, stated as Corollary 5.2.4 in [14]

Theorem 2.3.2 (Schleimer) *Let M be a closed orientable surface bundle which is irreducible. Let $\mathcal{T}$ be a 0-efficient triangulation of M. Then M has only finitely many surface bundle structures with strongly irreducible monodromy and for any of these a fiber can be found among the fundamental surfaces of $\mathcal{T}$.*

Proof. The argument is identical to that of Corollary 2.3.1 with a slight exception: Note that $M \backslash H$ is homeomorphic to $H \times I$ and all essential annuli are thus vertical. It follows that no exchange annulus, A can be essential. This is because $\partial_+ A$ and $\partial_- A$ are disjoint curves on H. ■

To reiterate, Theorem 2.3.2 applies to closed orientable 3-manifolds, but our needs require an analogous result where M has nonempty boundary. We are able to extend the result when M has a single torus boundary component.

Theorem 2.3.3 *Let M be a compact orientable irreducible 3-manifold with connected boundary component a torus. Suppose M is a surface bundle. Let $\mathcal{T}$ be a 0-efficient triangulation of M. Then a fiber for the bundle structure can be found among the fundamental surfaces of $\mathcal{T}$.*

We now sketch a proof of Theorem 2.3.3.

Proof. The proof follows that of Theorem 2.3.2. Pick a least weight representative of H. For $H = F + G$, any intersection curve of $F \cap G$ away from the boundary of M gives an exchange annuli which must not be essential for the same reasons as given above. Then by Lemma 2.3.2, H is not least weight, a contradiction. ■

The specification in Theorem 2.3.3 that M has a single boundary component is necessary. Given multiple boundary components, exchange bands can stretch from one component to another building an annulus that may be essential.

2.4 Crushing normal surfaces

Crushing a triangulation was first introduced by Jaco and Rubinstein [7]. The technique initially focused on crushing normal 2-spheres bounding a 3-cell to simplify a triangulation. This led immediately to the first practical implementation of 3-sphere recognition. Varying treatments have been described in the proceeding years. Our treatment will follow the

classic one as first developed by Jaco and Rubinstein. The full implementation works to crush normal surfaces other than normal 2-spheres. In fact we will be crushing normal tori, but this still will be a very special case. One that is purposefully built to be incredibly nice. The following results and discussion closely mirror [7] with only a slight translation to our notation.

Suppose $\mathcal{T}$ is a triangulation of a closed, orientable 3-manifold or a framed triangulation of the interior a compact, orientable 3-manifold M. Let S be a properly embedded normal surface in $\mathcal{T}$ and let X be the closure of a component of $M \backslash S$ not containing any vertices of $\mathcal{T}$. The technique of crushing gives sufficient conditions for constructing a nice ideal triangulation of the interior $\mathring{X}$. For our use of crushing, we start with a 3-manifold with boundary, and crush the boundary link arriving at an ideal triangulation with $\mathring{X}$ homeomorphic to $\mathring{M}$.

The union of S and $\mathcal{T}$ induces a cell decomposition, $\mathcal{C}$ on X. Because we required no vertex of $\mathcal{T}$ to be in X, there are induced cells of four types:

Definition 2.4.1 (Jaco-Rubinstein) *The four cell types in the induced cell decomposition $\mathcal{C}$ of X are: truncated tetrahedra denoted* ***cells of type I****; truncated prisms denoted* ***cells of type II****; triangular prisms denoted* ***cells of type III****; quadrilateral prisms denoted* ***cells of type IV****. See Figure 7.*

The identifications under crushing are suggested in Figure 7 and for our purposes they will work exactly as described, but care needs to be taken around the latter three cell types. Additionally we would like to use some of the language associated to crushing these types.

Definition 2.4.2 (Jaco-Rubinstein) *Four sided faces in $\mathcal{C}$ that are not in S are called* ***trapezoidal faces****.*

The above definition is to avoid confusion with the normal quadrilateral discs.

Definition 2.4.3 (Jaco-Rubinstein) *Define the* ***product region of*** *$\mathcal{C}$ as*

$$\mathbb{P}(\mathcal{C}) = \{\textit{edges in } \mathcal{C} \textit{ not in } S\} \cup \{\textit{all trapezoids of } \mathcal{C}\} \cup \{\textit{all cells of types III and IV of } \mathcal{C}\}.$$

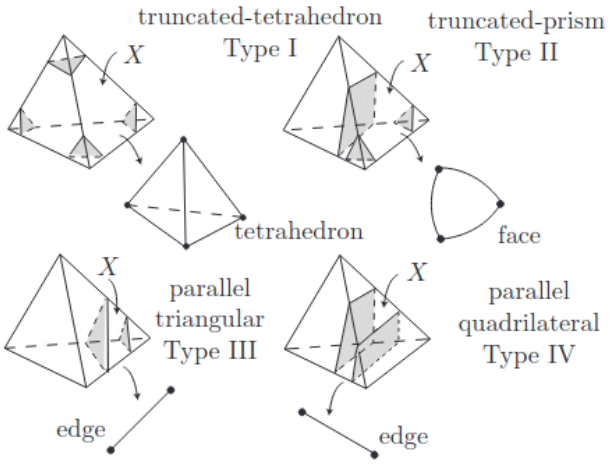

Figure 7: The four cell types before and after crushing [7].

We will later show, with our construction, that $\mathbb{P}(\mathcal{C}) \neq X$ and each component $\mathbb{P}_i$ of $\mathbb{P}(\mathcal{C})$ is a product I-bundle. Further, set $\mathbb{P}_i = K_i \times [0,1]$, where K_i is isomorphic to a subcomplex S. Let $K_i^\epsilon = K_i \times \{0\} \cup \{1\}$. We claim that each K_i^ϵ is simply connected (in our special case specifically).

Definition 2.4.4 (Jaco-Rubinstein) *Let $\mathbb{P}(\mathcal{C})$ be the product region of $\mathcal{C}$. If for each component written $\mathbb{P}_i = K_i \times [0,1]$ as above, K_i^ϵ is simply connected then we say that $\mathbb{P}(\mathcal{C})$ is a **trivial product region**.*

Each cell of type II has two hexagonal faces. It is clear from the cell decomposition of X that such a hexagonal face must be either identified to a cell of type I or another cell of type II.

Definition 2.4.5 (Jaco-Rubinstein) *Through these identifications of hexagonal faces we can trace a path of truncated prisms, called a **chain**. If the chain ends in a cell of type I, we say the chain **terminates**; otherwise we say the chain is a **cycle**.*

In our construction, we will see that there are no cycles of truncated prisms.

Collecting our assumptions we have: $X \neq \mathbb{P}(\mathcal{C})$, implying there are cells of type I; $\mathbb{P}(\mathcal{C})$ is a trivial product region; there are no cycles of truncated prisms. The implementation of

crushing under these assumptions will follow. Let the collection of truncated tetrahedra in X be given by $\{\overline{\Delta}_0, \ldots, \overline{\Delta}_{n-1}\}$. A face, $\overline{\sigma}_i$ of a truncated tetrahedron is either identified to another truncated tetrahedron or to a hexagonal face of a truncated prism. In the latter case we follow a finite length chain (in our case of length ≤ 3) of truncated prisms terminating in a truncated tetrahedron $\overline{\Delta}_j$'s hexagonal face $\overline{\sigma}_j$. We then have a natural identification $\overline{\sigma}_i \to \overline{\sigma}_j$. Note, it is possible $\overline{\Delta}_i = \overline{\Delta}_j$ but this causes no issues as the faces $\overline{\sigma}_i, \overline{\sigma}_j$ must be distinct. We thus have induced a face pairing on $\{\overline{\Delta}_0, \ldots, \overline{\Delta}_{n-1}\}$. The triangular faces of a type I cell lie in the normal surface S. We identify each such triangular face to a distinct point, yielding a tetrahedron $\tilde{\Delta}_i^*$, denote the face $\tilde{\sigma}_i$ to be the face induced from $\overline{\sigma}_i$. We then have a collection $\mathbf{\Delta}^* = \{\tilde{\Delta}_0^*, \ldots, \tilde{\Delta}_{n-1}^*\}$ with orientation induced by $\mathcal{T}$ and a family $\mathbf{\Phi}^*$ or orientation reversing homeomorphisms defined by the above induced face pairings. We therefore have a triangulation $\mathcal{T}^*$ as described in Section 1.1.

Definition 2.4.6 (Jaco-Rubinstein) *The constructed triangulation $\mathcal{T}^*$ is said to be the* ***crushing*** *of $\mathcal{T}$ along S.*

We refer to the function of crushing as the *crushing map* with the association $\mathcal{T} \to \mathcal{T}^*$. The following theorem from [7] shows the existence of crushing maps.

Theorem 2.4.1 (Jaco-Rubinstein) *Suppose $\mathcal{T}$ is a triangulation of a closed, orientable 3-manifold or an ideal triangulation of the interior of a compact orientable 3-manifold M. Suppose S is a normal surface in $\mathcal{T}$ and X the closure of a component of the complement $M \backslash S$ not containing any vertices of $\mathcal{T}$, $\mathcal{C}$ the induced cell decomposition of X. Suppose $\mathbb{P}(\mathcal{C})$ is a trivial product region. If $X \neq \mathbb{P}(\mathcal{C})$ and there are no cycles of truncated prisms, then $\mathcal{T}$ can be crushed along S to a triangulation $\mathcal{T}^*$ of $\mathring{X}$.*

In the above case we say that $\mathcal{T}$ admits a *combinatorial crushing along S*. The importance this construction has for our work lies in the existence of a one-to-one correspondance between the tetrahedra of $\mathcal{T}^*$ and the type I cells of $\mathcal{C}_X$.

2.5 Inflations

2.5.1 Frames

We now discuss a simple (if inefficient) method of constructing a frame for a triangulated torus. We also give further details regarding frames.

To build a frame, we begin with a triangulated torus S with triangulation T. We then consider the dual 1-skeleton of the triangulation, G. Because G is dual to a triangulation, G is a trivalent graph. Beginning with a vertex v in G, we perform a breadth first search until we arrive at a shortest cycle based at v, call it branch B_0'. The breadth first search method gives an orientation to B_0', by orienting each edge added away from the previously found edge. The complement $A = S \backslash B_0'$ is homeomorphic to an annulus. Let G' be obtained from (S, G) by doubling and cutting B_0', allowing an embedding of G' in A with the two copies of B_0' lying in the boundary components of A. We orient A by the induced orientation of the two copies of B_0' making a right hand twist around A, thus there is an upper ${B_0'}^+$ and lower ${B_0'}^-$ labeling of ∂A and two copies v^+ and v^- of v.

Because G and thus G' is trivalent, one of v^+, v^- will be of index 3, the other index 2. Assuming v^- is of index 2, beginning at v^-, move in accordance to the orientation along edge e' of ${B_0'}^-$ to an adjacent vertex and perform a breadth first search to reach v^+ while avoiding ${B_0'}^+$. Similarly if v^- is of index 3, we perform a breadth first search to find, not v^+ but the adjacent vertex contrary to the orientation of ${B_0'}^+$; we then add the edge, e'' connecting v^+, creating B_1^*. We always avoid ${B_0'}^-$ and ${B_0'}^+$ except with the previously described edges. We can thus identify ${B_0'}^- \to {B_0'}^+$, thus identifying the endpoints of ${B_1'}^*$ creating a cycle B_1' in G sharing a single edge, e the lift of e' or e'', with B_0'.

The constructions B_0', B_1' do create a cut set for S, however they are not in the 1-skeleton of T rather they lie in G. To remedy this we overlay T with B_0' and B_1'. Viewed as curves in S, B_0', B_1' meet the triangles of T in normal arcs. We can thus label the triangles of T with an s for short side at the vertex linked by an arc in B_i', and similarly label l for the opposing

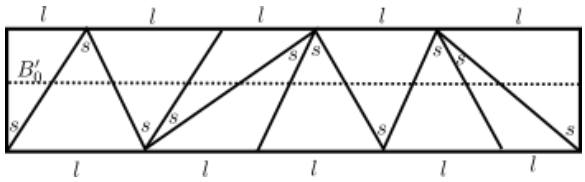

Figure 8: Labeling for projection of B_0'.

side (see Figure 8). We can then project B_i' onto the 1-skeleton of T, creating B_i as follows:

1. Using the orientation of B_i', place a transverse ν vector to B_i' on S.

2. Following the orientation of B_i', either exclusively in the positive or negative direction of ν, use the labelings s, l to project with the following instructions:

   (a) If the region is labeled s, the arc is identified with the linked vertex.

   (b) If the region is labeled l, the arc is identified with the opposite edge.

Notice that in step 2 above, either direction is allowed. The length of the two projections will differ by the magnitude $|s - l|$, thus whichever direction has the most s labels should always be preferred.

We now have branches B_0, B_1 which will be a frame proper. However, there is still a question about the intersection after the projection. This question is trivial away from edge $e = B_0' \cap B_1'$. It is easy to illustrate the projection of, e as seen in Figure 8, but more precisely, the projection moves full arcs over regions labeled l to edges in T. Because e is only half a normal arc, and together with B_0', B_1', e creates different respective normal arcs in both triangles of T it intersects, B_0', B_1' cannot have the same labelings in a respective triangle near e. Thus $B_0 \cap B_1$ is a single vertex of T, meaning we have a branch point of index 4 in our frame (which is preferred for our procedure in the next section).

The triangulations of surfaces we apply this technique to arise as vertex-linking surfaces in ideal triangulations. For an ideal triangulation with n tetrahedra there are at most $2n$ ideal vertices. Then for compact 3-manifold with torus boundary components, we can find the maximal length of such a constructed frame.

Remark 2.5.1 *Let $(\mathcal{T}^*, \Lambda)$ be a framed triangulation such that every vertex of $\mathcal{T}^*$ is ideal. If $|\mathcal{T}^*| = n$ then $len(\Lambda) < 8n$ and $\mathcal{C}(\Lambda) < 8n + 2n = 10n$.*

As each edge of ξ is a normal arc in the 2-skeleton of $\mathcal{T}^*$, there are $6n$ possible arcs. Additionally there are n edges at which there could be crossings. The bounds in Remark 2.5.1 are (gross) overestimates if any care is taken choosing a frame. Nevertheless the bounds are linear in terms of the number of tetrahedra in $\mathcal{T}^*$.

2.5.2 Inflating

We would like to describe an inverse of the crushing map. To that end an intuitive definition arises [7].

Definition 2.5.1 (Jaco-Rubinstein) *If $\mathcal{T}^*$ is an ideal triangulation of the interior of a compact 3-manifold M, an **inflation of** $\mathcal{T}^*$ is a minimal vertex triangulation $\mathcal{T}$ of M with normal boundary that admits a combinatorial crushing along ∂M for which the ideal triangulation obtained by crushing $\mathcal{T}$ along ∂M is the ideal triangulation $\mathcal{T}^*$ of $\mathring{M}$.*

In the above definition, it is meant to inflate all boundary components of $\mathcal{T}^*$. We can extend this definition to inflate only one boundary and be compatible with our notion of framed triangulations.

Definition 2.5.2 *Given a triangulation $\mathcal{T}_\xi$ with underlying topological space X where the interior of X is homeomorphic to the interior of a compact 3-manifold M. If $\mathcal{T}_\xi$ has real boundary, then we say that $\mathcal{T}_\xi$ is a **combinatorial inflation** if the boundary of M is normal in $\mathcal{T}_\xi$ and $\mathcal{T}_\xi$ admits a combinatorial crushing along ∂M yielding an ideal triangulation of the interior of M.*

Given a framed triangulation $(\mathcal{T}^*, \Lambda)$ with $\xi \in \Lambda$ a frame in S_{v_i} the vertex-link of ideal vertex v_i, $\mathcal{T}_\xi$ is the inflation occurring only at the ideal vertex S_{v_i}. The inflation triangulation $\mathcal{T}_\Lambda$ will then mean the triangulation obtained by inflating $\mathcal{T}^*$ at every ideal vertex with instructions given by Λ.

When we want to emphasize the underlying framed triangulation $\mathcal{T}^*$ we say that $\mathcal{T}_\xi$ is an inflation of $\mathcal{T}^*$. Otherwise we will say that $\mathcal{T}_\xi$ is an inflation triangulation. By the above definition, given a triangulation $\mathcal{T}_\xi$ it can be decided if $\mathcal{T}_\xi$ is a combinatorial inflation. First, each component of the boundary of a regular neighborhood of ∂M must be a normal surface (a boundary-link). The admission of a combinatorial crushing can be seen by Proposition 2.5.1:

Proposition 2.5.1 *Let $\mathcal{T}_\xi$ be a combinatorial inflation. For each ideal vertex, v_i of $\mathcal{T}_\xi$ let S_{v_i} represent the vertex-link of v_i and for every real boundary component B_j let S_{B_j} represent the boundary-link of B_j. Let $S = \sum_i S_{v_i} + \sum_j S_{B_j}$ be a normal sum. The surfaces $\{B_j\}$ are compatible thus S is well defined. Let X be the complement of S not containing any vertex of $\mathcal{T}_\xi$. Every tetrahedron of $\mathcal{T}_\xi$ contains exactly one cell of the induced cellulation of X.*

An inflation of an ideal triangulation $\mathcal{T}^*$ includes all of the tetrahedra of $\mathcal{T}^*$ then, as described below, tetrahedra are added based on information incoded in the frame Λ to arrive at a minimal vertex triangulation $\mathcal{T}_\Lambda$. To reiterate Definition 2.5.1, $\mathcal{T}_\Lambda$ will have normal boundary that admits a combinatorial crushing, mapping back exactly to $\mathcal{T}^*$. This relationship between crushing and inflation is illustrated in Figure 9. Although we will be focusing on inflating torus boundary, the notion of inflation does extend for any boundary component that is not a 2-sphere or $\mathbb{RP}^2$.

For inflations, a tetrahedron contains exactly one cell of X, the complement of S as in Proposition 2.5.1. We can then identify tetrahedra of $\mathcal{T}_\xi$ by the cell type of X found within.

Definition 2.5.3 *Let Δ_i be a tetrahedra of $\mathcal{T}_\xi$, S, X defined as above. If Δ_i contains a cell of type I, we say that Δ_i is a **type I tetrahedra**. If Δ_i contains a cell of type II, we say that Δ_i is a **type II tetrahedra**. If Δ_i contains a cell of type III, we say that Δ_i is a **type III tetrahedra**. If Δ_i contains a cell of type IV, we say that Δ_i is a **type IV tetrahedra**.*

For each inflated boundary component B_i of $\mathcal{T}_\xi$, there are exactly $4g-2$ type III tetrahedra where g is the genus of B_i. The chains of type II tetrahedra following the discussions in

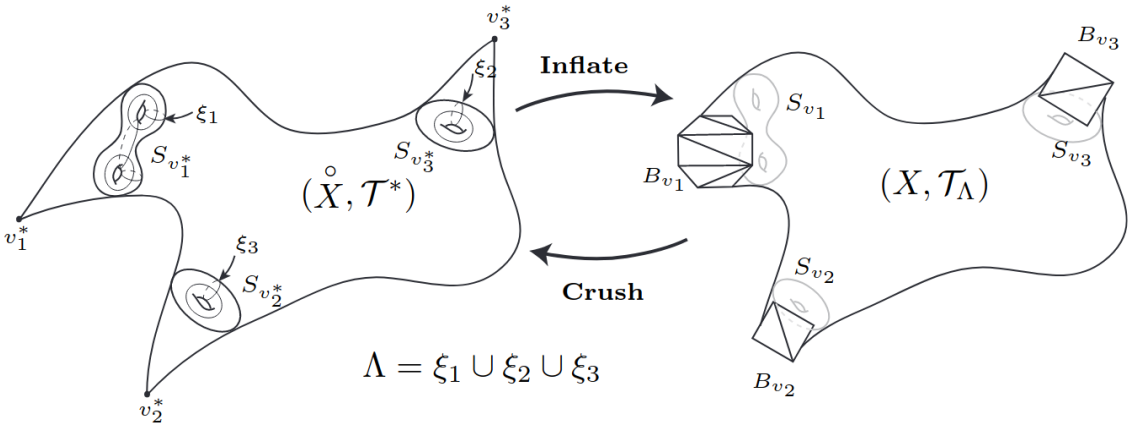

Figure 9: The inverse relationship between inflating and crushing the boundary [2].

Section 2.3 are at most length 3. We go into further detail regarding the classification of tetrahedra in inflation triangulations in Chapter 4.

Given the combinatorial definition of inflations we now present a procedure to construct an inflation given a framed triangulation. Our method for inflating ideal triangulations follows [7] except in those places where one is free to choose how to triangulate certain 3-cells as noted in the Introduction. The presentation is stated in a way to be compatible with REGINA[4]. We take as input an isomorphism signature as recognized by the low dimensional topology suite REGINA, which perfectly encodes the gluing information of an ideal triangulation of a cusped 3-manifold, M. See Burton [3] for more information on the isomorphism signature of a triangulation. We then require the triangulation to be oriented. We call the oriented triangulation complete with all gluing data $\mathcal{T}^*$. Where presenting gluing data, we use the notation from REGINA. We construct the vertex linking normal surface, L, oriented so that a positive normal vector to L points towards the ideal vertex(s) of M as in. From the edges of L we construct the frame, ξ as in Subsection 2.6.1. Give the branches orientations, and order them with a right hand rule such that if the fingers point in the direction of the orientation or branch 1 and thumb points in the direction of a positive normal vector to L, then the fingers curl in the direction of the orientation of branch 2. We can list the edges in order following the orientations of the branch. Each edge, E, in a

branch represents a normal arc in some pair of faces in $\mathcal{T}^*$. We choose the tetrahedron, Δ_i, with a left hand rule such that with fingers pointing in the direction of E and thumb in the direction of a positive normal vector to L, the fingers curl to point at Δ_i. We now represent E by a list $[\Delta_i, f_k, v_j]$ where Δ_i is the corresponding tetrahedron, v_j the vertex of Δ_i linked by E, and f_k the face of Δ_i containing E. Each branch B is represented as a list of edges e starting at the branchpoint and having order inherited by the branch.

It is here we first diverge (slightly) from the procedure in [7]. Before we begin inflating $\mathcal{T}^*$ we need to identify if the frame has any *crossings*. For each edge class, e in $\mathcal{T}^*$, give an orientation to e. Now sweep through the book of faces incident to e. As we sweep we create a 'word' of symbols; if a face contains a normal arc linking to vertex at the positive end of e add a '+', if a face contains a normal arc linking the negative end of e add a '$-$'. We now append the word to itself and call the result the *edge-word*. If no branchpoint of ξ is on e, then we say that there is a crossing at e if and only if the edge-word contains the pattern '$+-+$'. If e has a branchpoint, then orient e so that the branchpoint is at the positive end of e. We say that there is a branch crossing at e if the edge-word contains a '$-$' and does not contain the pattern '$--$'.

We can now begin inflating the faces of $\mathcal{T}^*$. For each edge e in each branch B we have the corresponding list $[\Delta_i, f_k, v_j]$, where v_j is labeled a, f_k labeled (abc). In $\mathcal{T}^*$ there is a corresponding tetrahedron Δ_i' such that Δ_i is glued to Δ_i' through face f_k, using the notation of REGINA, $(\Delta_i)(abc) \to (t_i')(a'b'c')$. We now add a new tetrahedron Δ_e so that a right hand twist around edge (01) sweeps from vertex 3 to 2. We remove the gluing $(\Delta_i)(abc) \to (\Delta_i')(a'b'c')$ and insert Δ_e with gluings $(\Delta_e)(123) \to (\Delta_i)(acb)$ and $(\Delta_e)(023) \to (\Delta_i')(a'c'b')$.

For those edge classes e in $\mathcal{T}^*$ that meet ξ yet do not present a crossing, e meets ξ in a valence 2 vertex, meeting edges e_i, e_{i+1}, we simply glue $\Delta_{e_i}, \Delta_{e_{i+1}}$ with the map $(\Delta_{e_i})(013) \to (\Delta_{e_{i+1}})(012)$.

For a crossing c, we have four edges $e_i, e_{i+1}, e_j, e_{j+1}$ from ξ incident to an edge e in $\mathcal{T}^*$. After inflating the faces containing e_i, e_{i+1} we add an edge to the branch containing

$e_j, e_{j+1} \to e_j, e_{j'}, e_{j+1}$ where $e_{j'}$ is the normal arc in the face shared by e_i, e_{i+1} linking the same vertex as linked by e_i, e_{i+1}.

At the branchpoint we add tetrahedra $\Delta_{b_1}, \Delta_{b_2}$ and create a *branch pyramid* with the gluing $(\Delta_{b_1}(023) \to (\Delta_{b_2})(013)$. We then make the identifications from the branches. Suppose that e_0, e_i are the first and last edges of branch 1 respectively and e_{i+1}, e_n are the first and last edges of branch 2. We then make the following identifications

$$(\Delta_{e_0})(012) \to (\Delta_{b_1})(213)$$
$$(\Delta_{e_i})(013) \to (\Delta_{b_2})(203)$$
$$(\Delta_{e_{i+1}})(012) \to (\Delta_{b_2})(213)$$
$$(\Delta_{e_n})(013) \to (\Delta_{b_1})(013)$$

If there is a branch crossing, suppose that edges $e_j, e_{j+1} \in \xi$ are the edges contributing the '$-$' symbols in the edge-word. Then there is a face in the branch pyramid above with normal arc γ such that adding the arc as $e_{j'}$ as in the case of a crossing above and inflating the edge will yield a branch crossing as in [7].

The above construction is specific in the sense that the branchpoint is always assumed to be of valence 4 as the frame is to be constructed by the means of Subsection 2.5.1. Further the analysis of edge-words is specific to the boundary link being a torus. That is, for non-toric boundary components the edge-word analysis must be modified. For the full treatment of inflating non-toric boundary see [7]. This construction does however have the benefit of being procedural enough to be given to REGINA to compute.

We notice that we can construct an inflation in linear time:

Remark 2.5.2 *Let $(\mathcal{T}^*, \Lambda)$ be a framed triangulation of M. Suppose $|\mathcal{T}^*| = n$. Then the complexity of the inflation $|\mathcal{T}_\Lambda| = n + \mathcal{C}(\Lambda) < 11n$ for sufficiently large n.*

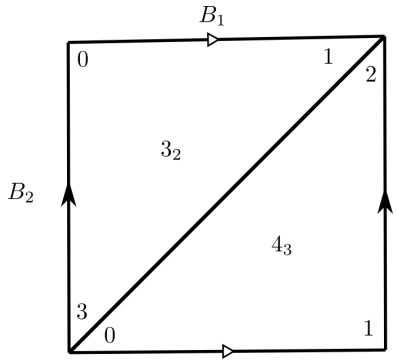

Figure 10: The vertex linking torus and chosen frame of 'fLAPcbbceeeemkjnb'.

2.5.3 Inflation examples

An *annanas*[6] refers to a subcomplex of an ideal triangulation consisting of two tetrahedra identified in such a way to be homeomorphic to $\mathbb{T}^2 \times [0,1) \backslash (point)$. This isolates a single ideal vertex v_a where the vertex-link consists of only two normal triangles. An example of such a triangulation $\mathcal{T}_A$, from isomorphism signature 'fLAPcbbceeeemkjnb' having five tetrahedra (gluings shown below) and two ideal vertices, the interesting vertex being $3(2), 4(3)$ after orientation (this orientation is given by REGINA's orient command for reproducibility).

tet	(012)	(013)	(023)	(123)
(0)	(1)(301)	(1)(023)	(2)(032)	(1)(132)
(1)	(2)(123)	(0)(120)	(0)(013)	(0)(132)
(2)	(3)(013)	(4)(012)	(0)(032)	(1)(012)
(3)	(4)(013)	(2)(012)	(4)(231)	(4)(230)
(4)	(2)(013)	(3)(012)	(3)(312)	(3)(302)

Table 1: Ideal triangulation of 'fLAPcbbceeeemkjnb' (the annanas being tetrahedra 3 and 4.

We now triangulate the vertex linking torus of $3(2), 4(3)$ and create the frame ξ as in Figure 10. The arrows represent the gluings of the torus as well as the orientation of our two branches. So branch 1 is given by $[[3,3,2]]$ and branch 2 by $[[3,1,2]]$. We then analyse the edge classes that meet ξ, in this case a singular edge labeled E_4 in Figure 10. We now inflate

the faces of $\mathcal{T}_A$ according to the two edges in ξ creating tetrahedra $(5), (6)$ in REGINA[4] with gluing data:

tet	(012)	(013)	(023)	(123)
(0)	(1)(301)	(1)(023)	(2)(032)	(1)(132)
(1)	(2)(123)	(0)(120)	(0)(013)	(0)(132)
(2)	(3)(013)	(4)(012)	(0)(032)	(1)(012)
(3)	(5)(231)	(2)(012)	(6)(312)	(4)(230)
(4)	(2)(013)	(5)(230)	(3)(312)	(6)(230)
(5)			(4)(301)	(3)(201)
(6)			(4)(312)	(3)(230)

Table 2: Inflating the edges.

Now we create the pyramid over the branchpoint with new tetrahedra $\Delta_{b_1}, \Delta_{b_2}$ labeled in Table 3 as $(7), (8)$ with gluing $(7)(013) \to (8)(023)$. The final step is to glue tetrahedra $(5), (6)$ (as they arrive from face inflation) to the pyramid:

tet	(012)	(013)	(023)	(123)
(0)	(1)(301)	(1)(023)	(2)(032)	(1)(132)
(1)	(2)(123)	(0)(120)	(0)(013)	(0)(132)
(2)	(3)(013)	(4)(012)	(0)(032)	(1)(012)
(3)	(5)(231)	(2)(012)	(6)(312)	(4)(230)
(4)	(2)(013)	(5)(230)	(3)(312)	(6)(230)
(5)	(7)(123)	(8)(103)	(4)(301)	(3)(201)
(6)	(8)(123)	(7)(023)	(4)(312)	(3)(230)
(7)		(8)(023)	(6)(013)	(5)(012)
(8)		(5)(103)	(7)(013)	(6)(012)

Table 3: The inflation of 'fLAPcbbceeeemkjnb'.

We now have a triangulation with one real boundary component (that we inflated) and

one ideal vertex. If we gave a frame for the ideal vertex we have a perfect example of a framed triangulation. The number of tetrahedra in the resulting triangulation is 9, the five original, one from each frame edge, and two from the branchpoint. This particular inflation is what we call in Chapter 4 a short inflation, where the number of tetrahedra corresponding to frame edges is two. We will see this is a best case scenario.

In the next example, we look at the Figure-8 knot complement. We begin by giving REGINA the isomorphism signature 'cPcbbbiht' and orient (in this case it is already oriented) to create our triangluation $\mathcal{T}$.

tet	(012)	(013)	(023)	(123)
(0)	(1)(203)	(1)(103)	(1)(102)	(1)(132)
(1)	(0)(203)	(0)(103)	(0)(102)	(0)(132)

Table 4: Initial ideal triangulation of 'cPcbbbiht'.

We then triangulate the vertex linking torus and create the frame ξ with branch 1 given by $[[0,1,0],[0,3,1],[0,3,2],[0,1,3]]$ and branch 2 by $[[0,3,0]]$. We then analyze the two edge classes of $\mathcal{T}$ labeled by their ends in Figure 2.1 by E_0, E_1. With the crossing data in hand we now inflate along the faces of $\mathcal{T}$ according to our five edges in F creating tetrahedra labeled in REGINA as $\Delta_2, \Delta_3, \Delta_4, \Delta_5, \Delta_6$ after which the gluing data is given by:

tet	(012)	(013)	(023)	(123)
(0)	(6)(123)	(1)(103)	(5)(231)	(1)(132)
(1)	(2)(203)	(0)(103)	(3)(032)	(0)(132)
(2)			(1)(102)	(5)(230)
(3)			(1)(032)	(4)(302)
(4)			(3)(231)	(6)(302)
(5)			(2)(312)	(0)(302)
(6)			(4)(231)	(0)(012)

Table 5: Inflating the edges.

The branchpoint lies on edge E_0, as there are no crossings at E_1 we simply glue $\Delta_{e_1} \to \Delta_{e_2}$ and $\Delta_{e_3} \to \Delta_{e_4}$ as above.

tet	(012)	(013)	(023)	(123)
(0)	(6)(123)	(1)(103)	(5)(231)	(1)(132)
(1)	(2)(203)	(0)(103)	(3)(032)	(0)(132)
(2)		(3)(012)	(1)(102)	(5)(230)
(3)	(2)(013)		(1)(032)	(4)(302)
(4)		(5)(012)	(3)(231)	(6)(302)
(5)	(4)(013)		(2)(312)	(0)(302)
(6)			(4)(231)	(0)(012)

Table 6: Connecting the branches.

We then build the branch pyramid creating tetrahedra $\Delta_{b_1}, \Delta_{b_2}$ labeled in REGINA $(7), (8)$. And as there is a branch crossing of type II we add $\Delta_{b'}$ labeled (9).

tet	(012)	(013)	(023)	(123)
(0)	(6)(123)	(1)(103)	(5)(231)	(1)(132)
(1)	(2)(203)	(0)(103)	(3)(032)	(0)(132)
(2)		(3)(012)	(1)(102)	(5)(230)
(3)	(2)(013)		(1)(032)	(4)(302)
(4)		(5)(012)	(3)(231)	(6)(302)
(5)	(4)(013)		(2)(312)	(0)(302)
(6)			(4)(231)	(0)(012)
(7)		(8)(023)		
(8)		(9)(321)	(7)(013)	
(9)				(8)(310)

Table 7: Adding the branch pyramid (tets 7 and 8) and crossing.

And finally glue the Δ_{e_i} to the inflated pyramid in order the frame edges e_i meet edge

E_0:

tet	(012)	(013)	(023)	(123)
(0)	(6)(123)	(1)(103)	(5)(231)	(1)(132)
(1)	(2)(203)	(0)(103)	(3)(032)	(0)(132)
(2)	(7)(123)	(3)(012)	(1)(102)	(5)(230)
(3)	(2)(013)	(9)(012)	(1)(032)	(4)(302)
(4)	(9)(013)	(5)(012)	(3)(231)	(6)(302)
(5)	(4)(013)	(9)(230)	(2)(312)	(0)(302)
(6)	(8)(123)	(7)(023)	(4)(231)	(0)(012)
(7)		(8)(023)	(6)(013)	(2)(012)
(8)		(9)(321)	(7)(013)	(6)(012)
(9)	(3)(013)	(4)(012)	(5)(301)	(8)(310)

Table 8: The inflation of 'cPcbbbiht'.

This gives us a triangulation of the knot exterior for the figure 8 knot with ten tetrahedra, two from the original triangulation, one from each of the five edges of F, two for the branch pyramid and one from the branch crossing. This is a minimal triangulation of the knot exterior, but is not the unique inflation with ten tetrahedra.

CHAPTER III

CLOSED NORMAL SURFACES AND INFLATIONS

In this chapter. we discuss the results of *Efficient triangulations and boundary slopes* [2], work joint with Jaco and Rubinstein. We extract only those results pertaining to closed normal surfaces in inflation triangulations. There are further results in [2] regarding annular-efficiency, end-efficiency and the finite-ness of boundary slopes supporting surfaces of bounded Euler characteristic. The reader is encouraged to find the paper as cited in the bibliography.

The following theorems completely describe the relationship between an ideal triangulation and its inflations with regards to closed normal surfaces. It is precisely because of this concise relationship demonstrated in Theorem 3.0.1 that inflations are used in the algorithms of [7] to modify a given ideal triangulation into a boundary-efficient triangulation. It is with this motivation and the same spirit that the work of Chapter 4 was carried out.

Lemma 3.0.1 (B-Jaco-Rubinstein) *Let M be a compact 3-manifold with nonempty boundary and $\mathcal{T}$ a triangulation of M with normal boundary. An embedded surface in $\mathcal{T}$ that contains all the quad types of a boundary-linking surface has that boundary linking surface as a component.*

Proof. Let B be a boundary linking surface, and let S be an embedded normal surface in $\mathcal{T}$ such that all quad types of B are present in S. Then the vector representatives $\vec{S}, \vec{B}$ are in the carrier of S. Since B has no more quad types than S, there is a normal surface R such that $kS = nR + mB$ for some positive integers k, n, m. Because B is a boundary link, we can move B by a normal isotopy so that it does not intersect R. Thus B is a component of kS, and therefore a component of S. ■

Lemma 3.0.2 (B-Jaco-Rubinstein) *Let M be a compact 3-manifold with nonempty boundary, no component of which is a 2-sphere. Suppose $(\mathcal{T}^*, \Lambda)$ is a framed triangulation of $\mathring{M}$, and $\mathcal{T}_\xi$ is an inflation of $\mathcal{T}^*$ along a frame ξ in Λ. The combinatorial crushing map determined by crushing $\mathcal{T}_\xi$ along ∂M takes a closed normal surface S in $\mathcal{T}_\xi$ to a closed normal surface S^* in $\mathcal{T}^*$; furthermore S and S^* are homeomorphic.*

Proof. Let X denote the component of the complement of the boundary linking surfaces that does not meet ∂M. Then X contains no vertices of $\mathcal{T}_\xi$ and has a cell-decomposition $\mathcal{C}$. By construction, this cell-decomposition combinatorially crushes along the boundary-linking surfaces to the framed triangulation $(\mathcal{T}^*, \Lambda)$.

Let S be some closed normal surface in $\mathcal{T}_\xi$. Because S is closed, we can move S via a normal isotopy so that it does not intersect the boundary-linking surfaces. Thus $S \subset X$.

If a normal quad or normal triangle of S is in a type I cell of $\mathcal{C}$, the crushing map takes the type I cell to an ideal tetrahedron of $\mathcal{T}^*$, and the normal cells of S in the type I cell are taken to normal cells in $\mathcal{T}^*$. See Figure 11. If a normal quad or normal triangle of S is in a type II cell, the crushing map takes the type II cell to a face in $\mathcal{T}^*$ and the normal cells are crushed to normal arcs in said face. The normal arcs in the hexagonal faces of the type II cells corresponds to where S meets these hexagonal faces and are matched under the crushing map from the various chains of type II cells. Arcs in the trapezoidal faces of the type II cells crush to points in the edges of the face to which the type II cells crush. See Figure 11. Lastly the normal cells of S in type III, IV cells of C must normal triangles and normal quads respectively. The crushing map takes each to a point in an edge of $\mathcal{T}^*$. It follows that the image of S under the crushing map is formed from a collection of normal triangles and normal quads of S that are in type I cells of $\mathcal{C}$, glued by identifications along their edges and gives a normal surface S^* in $\mathcal{T}^*$.

To see that S and S^* are homeomorphic, we observe that the inverse image (rel. the crushing map) of a point in the interior of a normal quad or normal triangle in S^* is a point in the interior of a normal quad or normal triangle in S. The inverse image of a point in

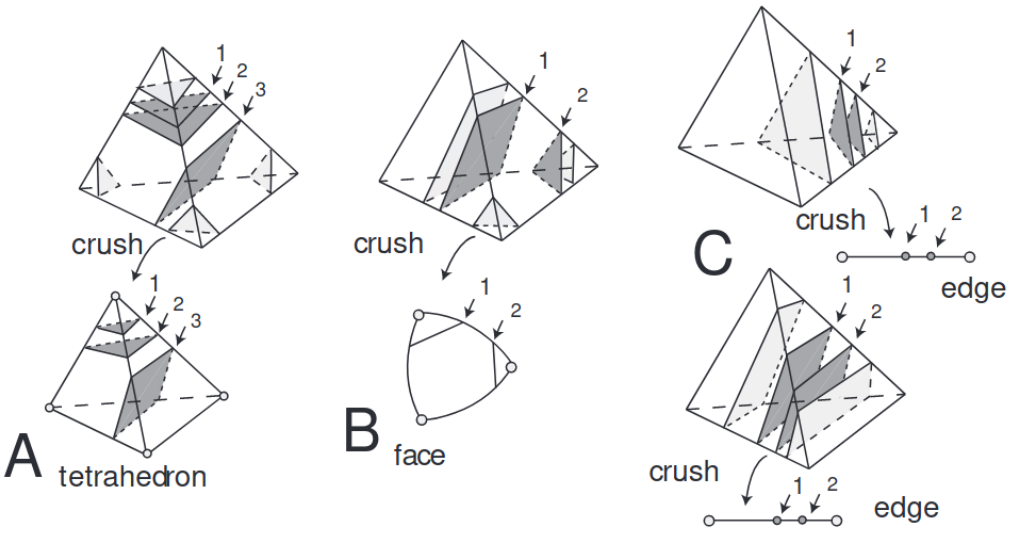

Figure 11: (A) Normal discs in a type I cell map to normal discs. (B) Normal discs in a type II cell map to normal arcs in a face. (C) Normal discs in type III and IV cells map to points on an edge [2].

an edge of S^* is either a point in an edge of S or a sequence of arcs in normal quads or normal triangles of S; due to $\mathcal{C}$ giving a combinatorial crushing there are no cycles of type II cells and so no cycles of cells of S in type II cells. The inverse image of a vertex of S^* is a horizontal cross section $K_i \times t$ in one of the component product pieces $\mathbb{P}_i = K_i \times I$ of the combinatorial product $\mathbb{P}(\mathcal{C}_X)$. Hence K_i is a contractible planar complex. Therefore, the inverse image of each point of S^* is a contractible planar complex and so the combinatorial crushing map gives a cell-like map from S to S^* and by a 2-dimensional version of [1, 15] S and S^* are homeomorphic. ■

Notice that the argument using the inverse images of points in S^* also shows that S^* is an embedded normal surface. The following theorem and its corollary are the main results for this chapter. They can be found as Theorem 3.5 and Corollary 3.6 in [2] respectively.

Theorem 3.0.1 (B-Jaco-Rubinstein) *Let M be a compact 3-manifold with nonempty boundary no component of which is a 2-sphere. Suppose $(\mathcal{T}^*, \Lambda)$ is a framed triangulation of $\mathring{M}$, and $\mathcal{T}_\xi$ is the inflation of $\mathcal{T}^*$ over some frame in Λ. The combinatorial crushing map determined by crushing $\mathcal{T}_\xi$ along ∂M induces a bijection between the closed normal surfaces in $\mathcal{T}_\xi$ and the closed normal surfaces in $\mathcal{T}^*$; furthermore, corresponding surfaces are homeomorphic.*

Proof. By Lemma 3.0.2 we only need to show that the combinatorial crushing induces a bijection between the closed normal surfaces of $\mathcal{T}_\xi$ and of $\mathcal{T}^*$.

We start with injectivity. Suppose S_1 and S_2 are distinct closed normal surfaces in $\mathcal{T}_\xi$. Since both are closed, we may assume that they do not meet any boundary-linking surface in $\mathcal{T}_\xi$. Let X denote the component of the complement of the boundary-linking normal surfaces in $\mathcal{T}_\xi$, which does not meet ∂M and let $\mathcal{C}_X$ denote the cell decomposition on X induced by $\mathcal{T}_\xi$. Then S_1 and S_2 are distinct normal surfaces in $\mathcal{C}_X$ and hence, have distinct normal coordinates. By Lemma 3.0.2 the combinatorial crushing map of $\mathcal{T}_\xi$ to $\mathcal{T}^*$ takes S_1 and S_2 to closed normal surfaces S_1^* and S_2^*, respectively. We must show that S_1^* and S_2^* have distinct normal coordinates.

Case 1: If S_1 and S_2 have distinct sets of normal disks in a type I cell of $\mathcal{C}_X$, then S_1^* and S_2^* have distinct normal discs in a tetrahedron of $\mathcal{T}^*$ and we are done.

Case 2: If S_1 and S_2 have distinct normal discs in a type II cell, say π, then they have distinct sets of normal arcs in a hexagonal face of π, which extend to distinct sets of normal arcs on all hexagonal faces of the type II cells in in the respective chain including π. This leads to a distinct set of normal discs in a type I cell in which the chain terminates and we have reduced to Case 1.

Case 3: If S_1 and S_2 have a distinct number of normal quads or triangles in a type III or IV cell, then S_1 and S_2 meet an entire product component $K_i \times I$ in a distinct number of horizontal slices. The vertical frontier of a product region $K_i \times I$ is made of trapezoidal faces which are paired with trapezoidal faces of type II cells. Thus we have that S_1 and S_2 must

meet a type II cell in distinct normal discs reducing to Case 2. Thus we have S_1^* and S_2^* are distinct and the correspondence is injective.

We now consider surjectivity. Suppose that S^* is a closed normal surface in $\mathcal{T}^*$. Consider how S^* meets a tetrahedron of $\mathcal{T}^*$. Each tetrahedron of $\mathcal{T}^*$ is the image of a single type I cell of $\mathcal{C}_X$ under the crushing map. So, there is a unique choice of normal cells in these type I cells mapping to normal cells of S^*. If σ^* is a face of a tetrahedron of $\mathcal{T}^*$ and σ^* meets S^*, then σ^* lifts to either a single face between two type I cells of $\mathcal{C}_X$, or a chain of type II cells between two type I cells. If there is a chain of type II cells, then of the three normal arcs in σ^*, each may correspond to only one normal quad type in any one type II cell in the chain. This determines a unique way to fill in normal discs extending the normal discs in type I cells. Finally, for each product component $K_i \times I$ there is a unique number of horizontal slices determined to complete a normal surface S in $\mathcal{T}_\xi$ that crushes to S^*. ■

In the supposition of Theorem 3.0.1 we have a framed triangulation with a framing Λ. For a given ideal triangulation there are many choices of framing giving distinct inflations $\mathcal{T}_\xi$. As the proof does not rely on the choice of Λ, for all inflations of $(\mathcal{T}^*, \Lambda)$ we have isomorphic sets of closed normal surfaces which are again isomorphic to the closed normal surfaces of $\mathcal{T}^*$. One sees immediately that analogous statements regarding normal surfaces with boundary can not be true. For instance, let M be a 3-manifold with one boundary component (not homeomorphic to a 2-sphere), $\mathcal{T}^*$ an ideal triangulation of $\mathring{M}$ with two frames Λ_1, Λ_2 such that the inflations $\mathcal{T}_{\xi_1}, \mathcal{T}_{\xi_2}$ have a different number of internal edges (occurring when the lengths of ξ_1, ξ_2 differ). For each internal edge, there is a normal thin edge-linking once punctured torus. Further these surfaces do not correspond to any spun-normal surface in $\mathcal{T}^*$. What analogies can be made are covered in Chapter 4. We end the chapter with results regarding efficiency of inflation triangulations.

Corollary 3.0.1 (B-Jaco-Rubinstein) *Suppose that $M \neq \mathbb{B}^3$ is a compact, irreducible and ∂-irreducible 3-manifold with nonempty boundary. Suppose that $\mathcal{T}^*$ is an ideal triangulation of $\mathring{M}$ with framing Λ, and $\mathcal{T}_\Lambda$ is an inflation of $\mathcal{T}^*$. Then there is a closed normal*

surface in $\mathcal{T}_\Lambda$ isotopic into ∂M but not normally isotopic into ∂M if and only if there is a closed normal surface in $\mathcal{T}^*$ that is isotopic into a vertex linking surface but is not normally isotopic into a vertex-linking surface.

Proof. Suppose that S and S^* are closed normal surfaces in $\mathcal{T}_\xi$ and $\mathcal{T}^*$ respectively. Then the closure of the components of the complement of S have a correspondence under the combinatorial crushing map and corresponding components are homeomorphic. Further, we have that the crushing map takes boundary-linking normal surfaces in $\mathcal{T}_\xi$ to vertex-linking surfaces in $\mathcal{T}^*$. Thus, if S is isotopic into ∂M, S is isotopic into a boundary-linking surface. Hence, S^* is isotopic to a vertex-linking surface in $\mathcal{T}^*$. Likewise if S^* is isotopic to a vertex-linking surface, through the homeomorphic components of the complements we have S is isotopic into a boundary-linking surface. ■

The following proposition does not appear in *Efficient triangulations and boundary slopes* though a portion of the proof is very similar to Proposition 4.5 therein.

Proposition 3.0.1 *Let M a compact, orientable 3-manifold with boundary, each component of which is a torus. Suppose that M is irreducible and ∂-irreducible. Let $\mathcal{T}^*$ be a triangulation of $\mathring{M}$ with ideal vertices. If $\mathcal{T}^*$ has a taut angle structure, then for any framing Λ the inflation $\mathcal{T}_\xi$ is 1-efficient and hence 0-efficient.*

Proof. By Proposition 2.3.1 $\mathcal{T}^*$ is 1-efficient. That is the only normal tori in $\mathcal{T}^*$ are vertex-linking and there are no normal 2-spheres. Then by Corollary 3.0.1 the only normal tori in $\mathcal{T}_\xi$ are boundary-linking. It is left to show $\mathcal{T}_\xi$ is 0-efficient. Suppose that S is a normal 2-sphere is $\mathcal{T}_\xi$. By Theorem 3.0.1 there is a corresponding normal 2-sphere S^* in $\mathcal{T}^*$ which is a contradiction to 1-efficiency. Likewise suppose that there is a normal disc D in $\mathcal{T}_\xi$ that is not vertex-linking. As M is ∂-irreducible D is isotopic into ∂M. A regular neighborhood of $D \cup \partial M$ then has two boundary components, a 2-sphere bounding a 3-cell and a torus T isotopic into ∂M. As $D \cup M$ forms a barrier, T shrinks to a normal torus that is isotopic

into ∂M but not normally isotopic, contradicting Corollary 3.0.1. Thus $\mathcal{T}_\xi$ is 0-efficient and 1-efficient. ■

The specificity of Proposition 3.0.1 regarding a taut triangulation is not needed, only that $\mathcal{T}^*$ is 1-efficient. This wording makes the proposition more directly applicable in the next chapter.

CHAPTER IV

FIBERS AS SPUN NORMAL SURFACES

4.1 2-3 Pachner moves

First we discuss the effects of "2-3" moves, with regards to the boundary linking surfaces. We will also mention the effects the moves may have on framings.

Definition 4.1.1 *Let $\mathcal{T}$ be a triangulation with two distinct tetrahedra Δ_i, Δ_j glued together at face σ. A* 2-3 move *is an operation on Δ_i, Δ_j at σ removing the face σ and the two tetrahedra and replacing them three tetrahedra $\Delta_m, \Delta_n, \Delta_l$ arranged around a new edge having endpoints the vertices of Δ_i, Δ_j not contained in σ.*

The benefits of 2-3 moves are two-fold. First:

Remark 4.1.1 *If S (spun-)normalizes in a (ideal) triangulation, then after a 2-3 move, S (spun-)normalizes in the resulting (ideal) triangulation. Abusing the name of the surface we call both normalizations of S simply S.*

We can easily verify this fact. Suppose that we wish to perform a 2-3 move at a face of the bipyramid formed by Δ_i, Δ_j. If S meets this bipyramid in a collection of normal discs, then S meets the resultant triangulation of the bipyramid by $\Delta_m, \Delta_n, \Delta_l$ in a collection of normal discs. This is illustrated in Figures 14-13. The second benefit being that the 2-3 move introduces new normal surfaces when compared to the pre-move triangulation. It is this addition that allows Theorem 3.0.1 and others to work. However it also allows for additional normal surfaces to arise, including for example a normal 2-sphere. Thus, we cannot say that after a 2-3 move whether or not the resulting triangulation is 0 or 1-efficient.

Let L be a link manifold with framed triangulation $(\mathcal{T}^*, \Lambda)$ and let $\mathcal{T}_\Lambda$ be an inflation of $\mathcal{T}^*$. As mentioned earlier, there is a natural identification of tetrahedra in $\mathcal{T}^*$ with tetrahedra in $\mathcal{T}_\Lambda$. This identification is most easily made through the cell decomposition of $\mathcal{T}_\Lambda$ induced by the union of all vertex linking tori. If $|\mathcal{T}^*| = n$ then there is an ordering of tetrahedra $\mathbf{\Delta} = \{\Delta_i\}_{0 \leq i < n}$. Then $|\mathcal{T}_\Lambda| = n + C$ where C is the complexity of the inflated frames; we can order the tetrahedra of $\mathcal{T}_\Lambda$ as the union of type I tetrahedra with the appropriate ordering inherited from $\mathcal{T}^*$, $\mathbf{\Delta}^* = \{\Delta_i\}_{0 \leq i < n}$, and the tetrahedra of types II, III and IV grouped together giving $\mathbf{\Delta}_\Lambda = \{\Delta_i\}_{n \leq i < n+C}$ corresponding to the inflated boundary. We see that $\mathbf{\Delta}_\Lambda$ has a distinct structure. Below the minimal triangulation of a component of ∂M lies two tetrahedra of type III, we call this the *branch pyramid*. The tetrahedra of type II are glued in such a way that in the trapezoidal faces, the normal arcs belonging to the normal quadrilateral are always glued. The effect is that the boundary linking surface has bands of quadrilaterals carried by the type II cells and type IV cells; type four cells give a place for the bands to cross over each other. We will see in Proposition 4.1.1 below that we can assume there are no crossings, hence we call the collection of type II cells carrying a band of quadrilaterals itself a *band*.

In this chapter we concern ourselves only with 2-3 moves taken where $\Delta_i, \Delta_j \in \mathbf{\Delta}_\Lambda$. We say that these 2-3 moves are *congruent*.

Proposition 4.1.1 *Let L be a 3-manifold with nonempty boundary each component of which is a torus with framed triangulation $(\mathcal{T}^*, \Lambda)$ and let $\mathcal{T}_\xi$ be an inflation of $\mathcal{T}^*$ of a boundary component of L. A congruent 2-3 move on $\mathcal{T}_\xi$ produces a triangulation $\mathcal{T}_{\xi'}$ that is a combinatorial inflation.*

Proof. The proof of Proposition 4.1.1 relies entirely on Figures 14, 13, and 12. To show that these figures suffice, we notice that in Figure 14 we replace two band tetrahedra with one, preserving the existence of a band of quadrilaterals; this move reduces the length of a band by one. In Figure 12, we remove the crossing tetrahedra (with a type IV cell) and replace it with three band tetrahedra, one in the orientation of the type II tetrahedron we applied the

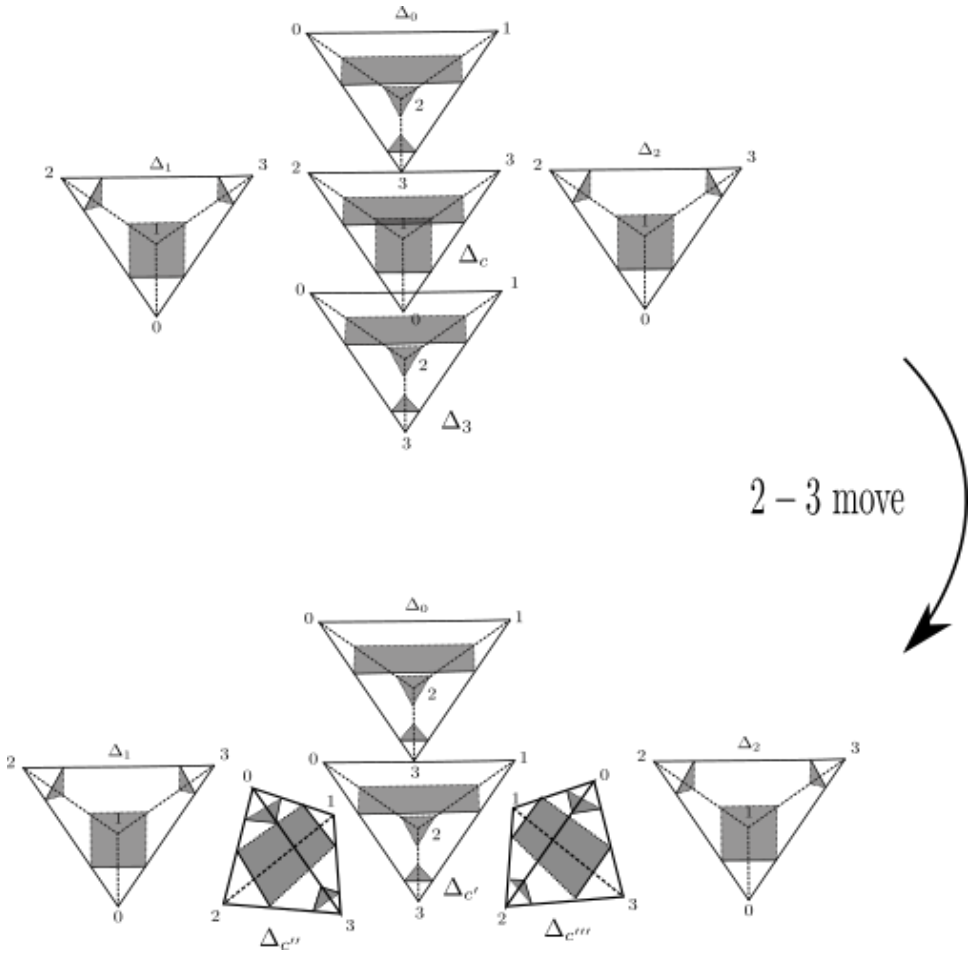

Figure 12: A 2-3 move at a crossing at face $(c)(023) \to (3)(201)$. Gluings are found in Tables 10 and 11. Shown is the boundary-linking surface.

2-3 move at, and the other two in the orientation of the other crossing quad band; this move eliminates crossings. Finally, in Figure 13, we remove a type II tetrahedron, shift the branch and add one type II tetrahedron to the other two bands (recall there can be three branches for a frame and hence three bands in $\mathcal{T}_\xi$). Thus, by tracking the boundary-link after a congruent 2-3 move, the resulting triangulation is a combinatorial inflation. To recover the frame in the idealtriangulation,$\mathcal{T}_B^*$, obtained by crushing the boundary, we can mark the normal arcs in all hexagonal faces carrying a band quadrilateral. It remains to show the effect of a 2-3 move at a site where there is a combinatorial crossing of two frames belonging to different boundary components. Notice had we inflated both frames, we would have had a site at

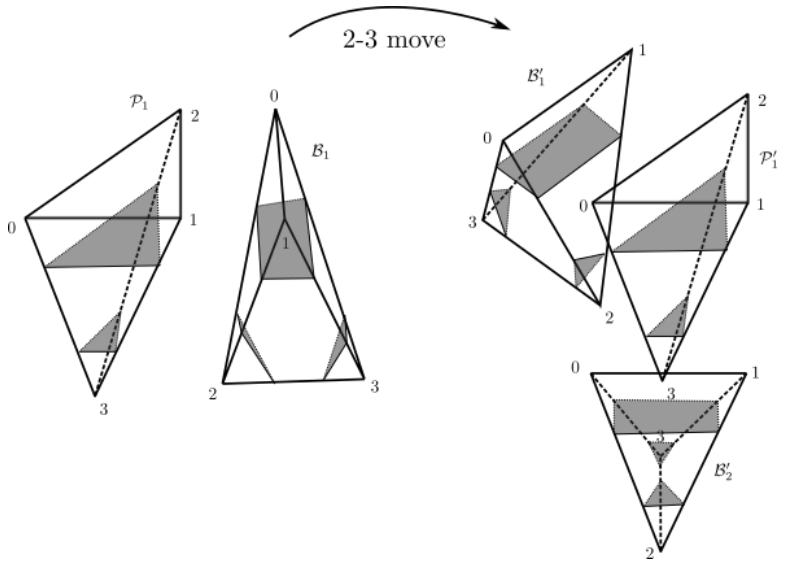

Figure 13: A 2-3 move between a type IV and type II tetrahedra at face $(\mathcal{P}_1)(123) \to (\mathcal{B}_1)(102)$. The resulting gluings are given in Figure 12.

which we could perform a 2-3 move illustrated in Figure 12. Thus we expect to add two edges to our un-inflated frame; these two edges are illustrated by the normal arcs belonging to the quadrilaterals on faces $(c'')(013)$ and $(c''')(012)$ in Figure 12. Giving the inflation $\mathcal{T}_{\xi'}$ of the framed triangulation $(\mathcal{T}_B^*, \Lambda)$ with $\xi' \in \Lambda$ ($\mathcal{T}_B^*$ is not the framed triangulation $\mathcal{T}^*$ we started with).

tet	(012)	(013)	(023)	(123)
(0)			(1)(013)	(2)(012)
(1)		(0)(023)		(2)(132)
(2)	(0)(123)			(1)(132)

Table 9: Gluings after a 2-3 move between type II tetrahedra.

■

As a result of Proposition 4.1.1, we can reduce an inflation of one torus boundary component so that it has two bands, each consisting of one type II tetrahedron.

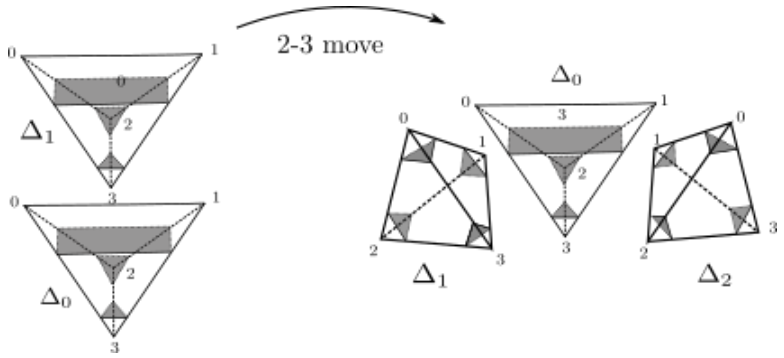

Figure 14: A 2-3 move at face $(0)(012) \to (1)(013)$ yields a single type II tetrahedron, Δ_0, and two type I tetrahedra, Δ_1, Δ_2. The resulting gluings are given in Table 9. Shown is the boundary-linking surface.

tet	(012)	(013)	(023)	(123)
(0)		$(c)(231)$		
(1)		$(c)(012)$		
(2)	$(c)(013)$			
(3)	$(c)(230)$			
(c)	(1)(013)	(2)(012)	(3)(201)	(0)(301)

Table 10: Gluings before a 2-3 move at crossing.

tet	(012)	(013)	(023)	(123)
(0)		$(c')(231)$		
(1)		$(c'')(210)$		
(2)	$(c''')(310)$			
(c')	(0)(013)		$(c'')(013)$	$(c''')(012)$
(c'')	(1)(310)	$(c')(023)$		$(c''')(132)$
(c''')	$(c')(123)$	(2)(210)		$(c'')(132)$

Table 11: Gluings after a 2-3 move at crossing.

We have then for a torus boundary component a standard picture of a short inflation, shown in Figure 15.

tet	(012)	(013)	(023)	(123)
$(\mathcal{P}_1')$		$(\mathcal{B}_2')(013)$	$(\mathcal{B}_1')(012))$	
$(\mathcal{B}_1')$	$(\mathcal{P}_1)(023)$	$(\mathcal{B}_2')(032)$		
$(\mathcal{B}_2')$		$(\mathcal{P}_1')(013)$	$(\mathcal{B}_1')(032)$	

Table 12: Gluings after a 2-3 move at a branch.

tet	(012)	(013)	(023)	(123)
$(\mathcal{P}_1)$		$(\mathcal{B}_2)(013)$	$(\mathcal{P}_2)(013))$	$(\mathcal{B}_1)(102)$
$(\mathcal{P}_2)$		$(\mathcal{P}_1)(023))$	$(\mathcal{B}_1)(103)$	$(\mathcal{B}_2)(102)$
$(\mathcal{B}_1)$	$(\mathcal{P}_1)(213)$	$(\mathcal{P}_2)(203)$		
$(\mathcal{B}_2)$	$(\mathcal{P}_2)(213)$	$(\mathcal{P}_1)(013)$		

Table 13: Gluings of the standard image of a short inflation.

Definition 4.1.2 *A **short inflation**, is an inflation triangulation having for each branch of inflated frame ξ a single type II tetrahedron.*

4.2 C-position

With this convention of $\mathbf{\Delta}^*$ and $\mathbf{\Delta}_\Lambda$ the normal coordinates in $\mathcal{T}_\Lambda$ coming from normal discs lifting to $\mathbf{\Delta}^*$ correspond to normal coordinates in $\mathcal{T}^*$, likewise for Q-coordinates. That is for a normal surface S in $\mathcal{T}_\Lambda$, if x_i is the Q-coordinate representing a class of normal quads in a tetrahedron $\Delta_j \in \mathbf{\Delta}^*$ there is a corresponding Q-coordinate representing the appropriate class of normal quads in $\Delta_m \in \mathbf{\Delta}$. We have chosen the naming convention so that $m = j$ and x_i is now the appropriate Q-coordinate in $\mathcal{T}^*$.

In the same vein let e_k be an edge in $\mathcal{T}_\Lambda$. Then we rewrite the Q-mathcing equation corresponding to e_k as

$$\sum_{i=1}^{3n+3C} \epsilon_{k,i} x_i = L^*(e_k) + L_\Lambda(e_k) = 0.$$

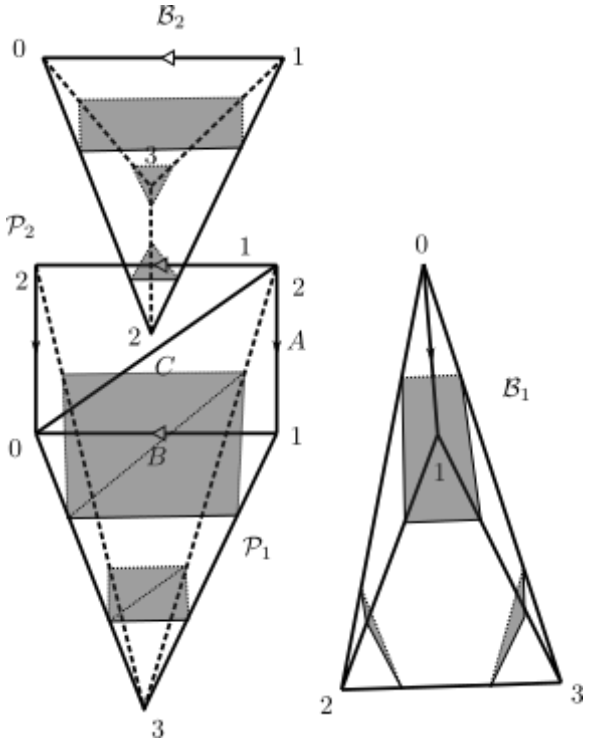

Figure 15: The standard inflated boundary in a short inflation. Gluings are given in Table 13.

Where

$$L^*(e_k) = \sum_{x_i \subset \Delta \in \mathbf{\Delta}^*} \epsilon_{k,i} x_i$$

$$L_\Lambda(e_k) = \sum_{y_j \subset \Delta \in \mathbf{\Delta}_\Lambda} \epsilon_{k,j} y_j.$$

Hence we write the vector representation of S as $\vec{S}_Q = (x_1, x_2, \cdots, x_{3n}, y_1, \cdots, y_{3C})$.

Let B be a boundary component of M, and $\mathcal{T}_\Lambda$ and inflated triangulation of M. Let $(\mathcal{T}, \Lambda')$ be a triangulation obtained from $\mathcal{T}_\Lambda$ by crushing the boundary link of B. We say that a normal surface S in $\mathcal{T}_\Lambda$ is *compatible with crushing* (wrt B) if there is a (spun-)normal surface S' in $\mathcal{T}$ where the Q-coordinates $\vec{S'}_Q = (x_1, x_2, \cdots, x_{3n})$ where x_i is exactly the entry from $\vec{S}_Q = (x_1, x_2, \cdots, x_{3n}, y_1, \cdots, y_{3C})$. We say that S *survives crushing* if S' is homeomorphic to S.

Definition 4.2.1 *Let Σ be the boundary-linking surface normal isotopic into B. If the normal surface S does not contain a normal quadrilateral type incompatible with Σ, then S is said to be in* ***C-position at Σ*** *or simply in C-position when the boundary component is understood.*

Lemma 4.2.1 *Let L be a 3-manifold with nonempty boundary, each component of which is a torus. Let $(\mathcal{T}^*, \Lambda)$ be a framed triangulation of the interior of L and let $\mathcal{T}_\Lambda$ be an inflation of $\mathcal{T}^*$. Let S be a normal surface in $\mathcal{T}_\Lambda$, with boundary no component of which is nullhomotopic in ∂L. Let Σ be some boundary linking torus normal isotopic into boundary component B. If S is in C-position at Σ, then S survives crushing along Σ.*

Proof. Given S a normal surface in $\mathcal{T}_\Lambda$, we write $\vec{S}_Q = (x_1, x_2, \cdots, x_{3n}, y_1, \cdots, y_{3C})$. Define $v = (x_1, x_2, \cdots, x_{3n})$, we wish to show v is the vector representation of some normal surface S' in $\mathcal{T}^*$. Let e_k be an edge in $\mathcal{T}^*$ and $\{\widehat{e_k^i}\}$ the lifts of e_k in $\mathcal{T}_\Lambda$ w.r.t the crushing map. The crushing map removes tetrahedra in $\mathbf{\Delta}_\Lambda$ and identifies faces of $\Delta_i \in \mathbf{\Delta}^*$ incident to $\widehat{e_k^i}$ forming e_k. The result on the Q-matching equations of e_k is

$$\sum_{j=1}^{3n} \epsilon_{k,j} x_j = \sum_{\widehat{e_k^i}} L^*(\widehat{e_k^i}) = -\sum_{\widehat{e_k^i}} L_\Lambda(\widehat{e_k^i}) \tag{4.2.1}$$

That is if

$$\sum_{\widehat{e_k^i}} L_\Lambda(\widehat{e_k^i}) = \sum_{\widehat{e_k^i}} \sum_{y_j \subset \Delta \in \mathbf{\Delta}_\Lambda} \widehat{\epsilon_{k,j}^i} y_j = 0 \tag{4.2.2}$$

then the conclusion will hold. In the case that e_k lifts to a unique edge $\widehat{e_k}$ not contained any $\Delta \in \mathbf{\Delta}_\Lambda$, Equation 4.2.2 holds as each $\widehat{\epsilon_{k,j}} = 0$. Otherwise e_k lifts to a collection (possibly unique) $\widehat{e_k}$ incident to tetrahedron(a) in $\mathbf{\Delta}_\Lambda$. We will show for each appropriate quadrilateral in each tetrahedra in $\mathbf{\Delta}_\Lambda$ the net sum for each corresponding $\widehat{\epsilon_{k,j}^i} = 0$ implying Equation 4.2.2. In Figure 16 we see a compatible normal quadrilateral and the two possible liftings of e_k.

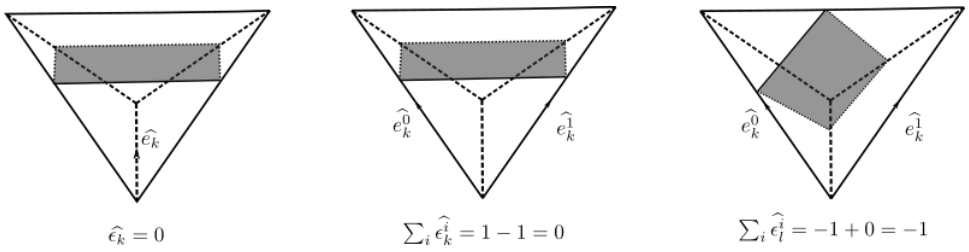

Figure 16: Two possible liftings of e_k in a type II tetrahedra with compatible and incompatible quads.

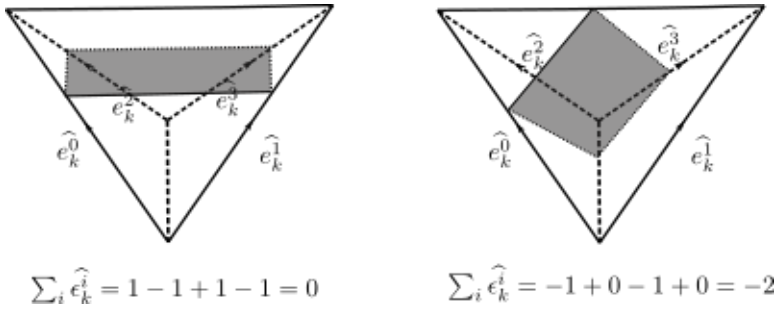

Figure 17: Compatible and incompatible quad in a type IV tetrahedra.

In a type IV tetrahedron there is in only one possible scenario for the lifts of e_k shown in Figure 17 below.

Finally in a type III tetrahedron there is only one possible case for the lifts of e_k shown in Figure 18. All quadrilateral types are compatible with Σ and the equations are symmetric.

Thus for each tetrahedron in $\mathbf{\Delta}_\Lambda$ corresponding to the inflation of B, a compatible quadrilateral type nets zero to the sum

$$\sum_{\widehat{e_k^i}} \sum_{y_j \subset \Delta \in \mathbf{\Delta}_\Lambda} \widehat{\epsilon_{k,j}^i} y_j$$

hence Equation 3.2.1 holds. Thus we have the coordinates of v satisfying the collection of Q-matching equations in $\mathcal{T}^*$ implying there is a (spun-)normal surface S' with v a Q-vector representation. We now have S' is compatible with crushing, it remains to show $S' \cong S$.

As the boundary component B has been crushed to a point, we have an ideal vertex and S' spins to B at said ideal vertex. Create S^- from S by removing all normal discs that are incident to B. This leaves the normal discs in Δ^* and those in Δ_Λ at other irrelevant

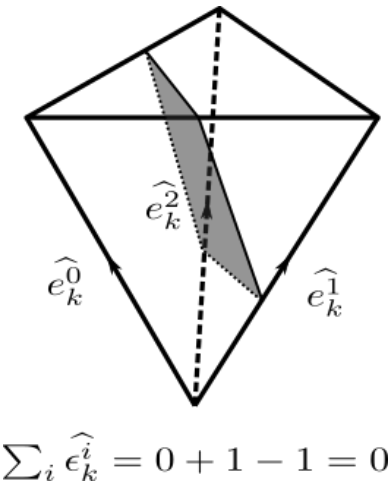

Figure 18: Normal quadrilateral in a type III tetrahedra.

boundary components. The normal quads in S^- correspond bijectively to the normal quads of S'. The collection of normal discs removed from S deformation retract to components of ∂S, hence we have removed a regular neighborhood of the self same components of ∂S. Thus $S^- \cong S$. But S^- is precisely what is left over from S after crushing B, thus S^- is a core of S'. Hence $S^- \cong S'$ completing the proof. ■

Notice that for a closed normal surface S in an inflation $\mathcal{T}_\xi$, S is necessarily in C-position, thus agreeing with the results of Theorem 3.0.1.

4.3 Main Results

Before proving the main theorems, we give some final required lemmas. These lemmas are included in this section as their own proofs match the flavor of the proofs of the main theorems.

First we step back to normal arcs on a 2-manifold. The proof of the following lemma relies solely on knowledge of slopes on a torus.

Lemma 4.3.1 *(**Torus Arc Lemma**) Let $\mathcal{T}$ be the triangulation of a the torus $\mathbb{T}^2$ consisting of two triangles. Let s be a connected simple closed curve on $\mathbb{T}^2$ that is not nullhomoptic.*

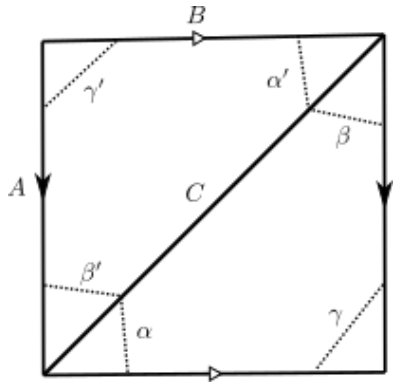

Figure 19: Normal arc classes on the minimal vertex triangulation of the torus.

Then s normalizes such that one of the pairs $(\alpha, \alpha'), (\beta, \beta'), (\gamma, \gamma')$ of normal arcs as shown in Figure 19 is $(0, 0)$.

Proof. A slope on $\mathbb{T}^2$ can be identified by a triplet (p, q, r) representing intersection numbers of the curve s with the edges A, B, C in Figure 19. Since s is assumed to not be nullhomotopic we can assume up to a homeomorphisim of $\mathbb{T}^2$ to itself that

$$p < q < r$$

$$r = p + q$$

$$\gcd(p, q) = 1.$$

The last line of the above equation follows from s being connected. If all three pairs are nonzero this gcd argument is violated. It is possible that two pairs, say $(\beta, \beta') = (\gamma, \gamma') = (0, 0)$. Then $(\alpha, \alpha') = (1, 1)$, also following from the gcd agrument. ■

It follows from Lemma 4.3.1 that a normal curve in the two triangle triangulation of $\mathbb{T}^2$ can be determined by a triplet (α, β, γ) where one of α, β, γ must be zero if the curve is not boundary linking. If one of p, q, r is zero we must have a triplet of the form $(1, 1, 0)$ up to permutation and the curve is homotopic to an edge A, B, C. With respect to the standard representation of a short inflation, we will always mean edge C to be the edge in the boundary of the branch pyramid having order 2, while edges A, B are the same up to symmetry.

Our final lemma is the first to yield a surface in C-position. It is in this same vein of observing the quadrilaterals in a short inflation in C-position that we will also prove the main theorems.

Lemma 4.3.2 *Let L be a 3-manifold with nonempty boundary, each component of which is a torus. Let $\mathcal{T}^*$ be an ideal triangulation of the interior of L. Let Λ be a collection of frames such that for some frame $\xi \in \Lambda$ at boundary cusp B, the inflation $\mathcal{T}_\xi$ is a short inflation. Let S be a normal surface (perhaps spinning around boundary components other than B) that meets B in a single simple closed curve that is not nullhomotopic. If S has an incompatible quad type with respect to the boundary link Σ in one band tetrahedra at B, then it must have an incompatible quad type in both bands.*

Proof. The following is a proof by contradiction. Using the naming conventions of Figure 15, assume that there is an incompatible quad type in $\mathcal{B}_2$. First we assume that $\mathcal{B}_1$ has no normal disk types incident to B the component of ∂L. Then by the intersection numbers on the triangulation of the boundary torus, the boundary slope of S, s, must be homotopic to either A or B, and we can determine there is no combination of normal discs in the complex $\mathcal{P}_1 \cup \mathcal{P}_2$ that is carried by this slope as shown in Figure 20 (the arcs on faces $(\mathcal{P}_1)(013)$ and $(\mathcal{P}_2)(123)$ are determined by the quad in $\mathcal{B}_2$). Now we assume $\mathcal{B}_1$ has some normal triangle types (possibly both) incident to the boundary B. If there are no normal quadrilaterals in $\mathcal{P}_1$ or $\mathcal{P}_2$, we have arcs of type γ', α', and β, contradicting the Torus Arc Lemma. Without loss of generality, assume the normal quadrilateral type in $\mathcal{B}_2$ separates edges (03) and (12). Let $y_{\mathcal{B}_2}$ represent the number of quadrilaterals of this type. Let $x_{i,\mathcal{B}_j}$ represent the number of normal triangles in $\mathcal{B}_j$ linking vertex i. Finally let x_θ, y_θ represent the number of normal triangles and normal quadrilaterals respectively having normal arc type $\theta \in \{\alpha, \alpha', \beta, \beta', \gamma, \gamma'\}$ as implied by Figures 15 and 19. We then have the following system of linear equations arising from the gluings of normal discs incident to the boundary

B:

$$\begin{aligned}
x_{0,\mathcal{B}_2} + y_{\mathcal{B}_2} &= x_{\gamma'} + y_{\alpha'} \\
x_{1,\mathcal{B}_2} + y_{\mathcal{B}_2} &= x_{\gamma} + y_{\alpha} \\
x_{1,\mathcal{B}_2} &= x_{\alpha'} + y_{\gamma'} \\
x_{0,\mathcal{B}_2} &= x_{\alpha} + y_{\gamma} \\
x_{0,\mathcal{B}_1} &= x_{\beta} + y_{\gamma} \\
x_{0,\mathcal{B}_1} &= x_{\gamma'} + y_{\beta'} \\
x_{1,\mathcal{B}_1} &= x_{\gamma} + y_{\beta} \\
x_{1,\mathcal{B}_1} &= x_{\beta'} + y_{\gamma'} \\
x_{\alpha} + y_{\beta} &= x_{\beta'} + y_{\alpha'} \\
x_{\beta} + y_{\alpha} &= x_{\alpha'} + y_{\beta'}
\end{aligned} \tag{4.3.1}$$

The Torus Arc Lemma gives three additional equations:

$$\begin{aligned}
x_{\alpha} + y_{\alpha} &= x_{\alpha'} + y_{\alpha'} \\
x_{\beta} + y_{\beta} &= x_{\beta'} + y_{\beta'} \\
x_{\gamma} + y_{\gamma} &= x_{\gamma'} + y_{\gamma'}
\end{aligned} \tag{4.3.2}$$

The assumption that the boundary curve of S is connected and not nullhomotopic means that exactly one of the equations from 4.3.2 is equal to zero. As the solution each of x_i, y_j must be nonnegative integers, this implies for example $x_\alpha = y_\alpha = x_{\alpha'} = y_{\alpha'} = 0$. Under these constraints (even ignoring the Quadrilateral Condition on $\mathcal{P}_1, \mathcal{P}_2$) the system given in 4.3.1 has a solution (even amongst the Reals) only when $y_{\mathcal{B}_2} = 0$, a contradiction. ■

The statement of Lemma 4.3.2 has been made cumbersome to deal with the extra complexity added by referring to manifolds with multiple torus boundary components. When the boundary is connected, the statement is much clearer and follows as a corollary:

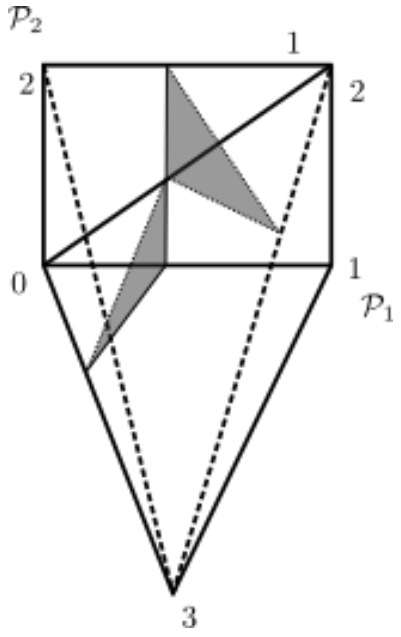

Figure 20: The boundary slope carrying no solution of normal discs when constrained by the normal arcs on $(\mathcal{P}_1)(013)$ and $(\mathcal{P}_2)(012)$.

Corollary 4.3.1 *Let K be a 3-manifold with nonempty connected boundary a torus. Let $\mathcal{T}^*$ be an ideal triangulation of the interior of K. Let ξ be a frame such that $\mathcal{T}_\xi$ is a short inflation. Let S be a normal surface that meets B in a single simple closed curve. If for one of the bands of $\mathcal{T}_\xi$, S has no incompatible quads, then S is in C-position.*

We now have the tools to prove the first of the main results. We deal specifically with embedded surfaces in which ∂S is connected.

Theorem 4.3.1 *Given a 3-manifold M with connected boundary a torus, let S be a properly embedded incompressible, ∂-incompressible surface in M with one boundary component. If ∂S is not nullhomotopic, then there exists an ideal triangulation of the interior of M in which S spun-normalizes.*

Proof. Let a framed triangulation $(\mathcal{T}^*, \xi)$ of the interior of M be given. We first construct the inflation $\mathcal{T}_\xi$. By Proposition 4.1.1 we may assume that $\mathcal{T}_\xi$ is a short inflation. As S is incompressible and ∂-incompressible, by Theorem 2.2.3 it normalizes in $\mathcal{T}_\xi$. If the

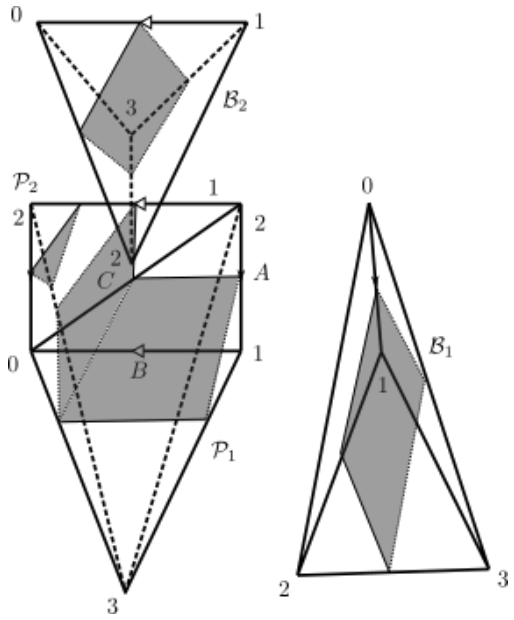

Figure 21: The normal triangle in $\mathcal{P}2$ is forced by the normal arc in $(\mathcal{B}_1)(013)$. Thus γ', β, α' are present.

normalization of S is in C-position we are done. Otherwise by Corollary 4.3.1 we can assume for both bands in the short inflation $\mathcal{T}_\xi$, S have an incompatible quad type. Up to symmetry we can assume the incompatible quad type found in $\mathcal{B}_1$ separates the edges (02) and (13) and the icompatible quad type in $\mathcal{B}_2$ separates the edges (03) and (12). Referring to the naming convention in Figure 19 we break the proof into cases based on which of the arcs α, β, γ carry normal quads in the branch pyramid (due to reflection symmetry, this will cover the possibilities for α', β', γ' carrying normal quads) and finally the case when there are no normal quads in the branch pyramid.

Case 1: We first consider the case when the normal arc class β carries normal quadrilaterals. Due to rotational symmetry this also covers the case of α carrying normal quads. We further break this case into subcases based on which of α', β', γ' carry quads in $\mathcal{P}_2$.

Subcase 1: When β and α' carry normal quad types, the incompatible quad type in $\mathcal{B}_1$ marks $\mathcal{P}_2$ in such a way that forces a normal triangle with arc γ'. This contradicts the Torus Arc Lemma. This is illustrated in Figure 21.

Subcase 2: When β and γ' carry normal quad types, we have markings on $\mathcal{B}_1, \mathcal{B}_2$ that must be pushed to the boundary as normal triangle types which then mark all side faces of $\mathcal{P}_1, \mathcal{P}2$ with normal arcs. As a normal quad type has been selected for $\mathcal{P}_1, \mathcal{P}_2$, these normal arcs must carry normal triangles having arc types of α'. This contradicts the Torus Arc Lemma.

Subcase 3: For the final subcase we will include both when β' carries a normal quad and when there are no normal quad types in $\mathcal{P}_2$. An example is shown in Figure 22. It is important to note the number of quads s in $\mathcal{B}_1$ must be greater than the number r in $\mathcal{P}_1$, otherwise the push off of the boundary curve into the normal discs would not be compact, a contradiction. Both instances can give an admissible normal surface and both are handled the same way. Dependent on the incompatible quad type found in $\mathcal{B}_1$ and $\mathcal{B}_2$, a 2-3 move between $\mathcal{B}_1$ and $\mathcal{P}_1$ or $\mathcal{P}_2$, or between $\mathcal{B}_2$ and $\mathcal{P}_2$ or $\mathcal{P}_1$ will (using Figure 13 as guide) make an additional type II tetrahedron in the band corresponding to $\mathcal{B}_2$ with an incompatible quad and a new band without an incompatible quad. An example is shown in Figure 22. Now by Proposition 4.1.1 we can perform a 2-3 move between the type II tetrahedra in the band of length 2 to arrive at a short inflation. As the 2-3 move was local, the other band still has no incompatible quads, so by Corollary 4.3.1 S must be in C-position.

tet	(012)	(013)	(023)	(123)
$(\mathcal{P}_1)$		$(\mathcal{B}_2)(013)$	$(\mathcal{B}_1')(012)$	$(\mathcal{P}_2')(023)$
$(\mathcal{P}_2')$		$(\mathcal{B}_1')(013)$	$(\mathcal{P}_1)(123)$	$(\mathcal{B}_2')(102)$
$(\mathcal{B}_1')$	$(\mathcal{P}_1)(023)$	$(\mathcal{P}_2')(013)$	$(\mathcal{B}_2')(132)$	
$(\mathcal{B}_2)$	$(\mathcal{B}2')(013)$	$(\mathcal{P}_1)(013)$		
$(\mathcal{B}_2')$	$(\mathcal{P}_2')(213)$	$(\mathcal{B}_2)(012)$		$(\mathcal{B}_1')(132)$

Table 14: Gluings after the 2-3 move in Figure 22

Case 2: We now consider when γ carries a normal quad. When β' or α' also carries a quad, we reduce the problem to Case 1: Subcase 2. We then only need to consider when γ' carries

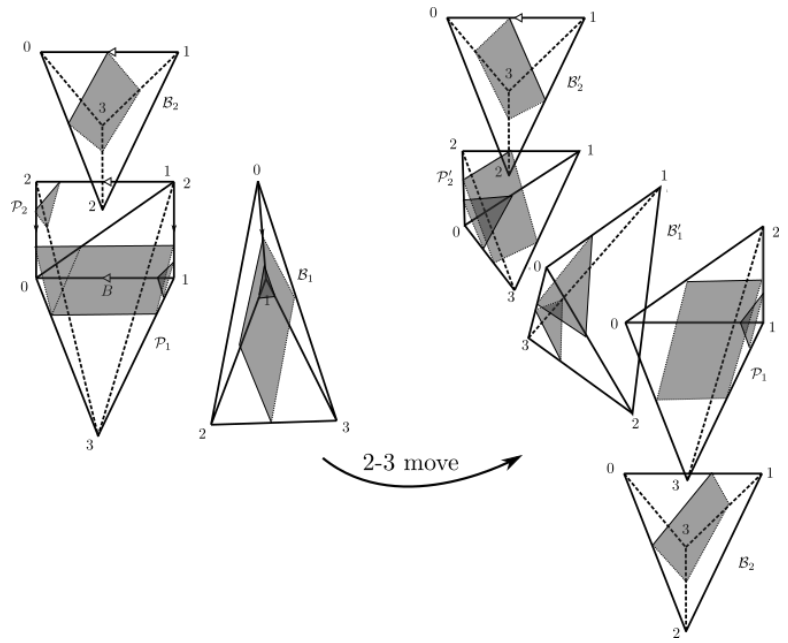

Figure 22: A 2-3 at $(\mathcal{B}_1)(013) \to (\mathcal{P}_2)(203)$. The gluings on the left are given in Table 13 and those on the right given in Table 14

a normal quad type or when $\mathcal{P}_2$ has no normal quad types.

Subcase 1: When γ' carries a normal quad we can again have an admissible normal surface. This however is more constrained than Case 1: Subcase 3. By adding any normal triangle type incident to the boundary in either $\mathcal{P}_1$ or $\mathcal{P}_2$, we mark additional edges on $\mathcal{B}_1$ or $\mathcal{B}_2$ that push up to arcs β, α' contradicting the Torus Arc Lemma. Thus we can only have the normal arcs γ, γ' present on the boundary and we have exactly the configuration shown in Figure 23. All 2-3 moves at the branch pyramid yield the same result up to symmetry (shown in Figure 23, the new band $\mathcal{B}_1'$ has no incompatible quadrilateral type and the additional type II tet added to the other band has an incompatible quad type; Thus after a 2-3 move shortening the band of length 2, by Corollary 4.3.1 S is in C-position.

Subcase 2: When $\mathcal{P}_2$ has no normal quad types, we again arrive at a contradiction by pushing down the normal arc and building necessary normal triangles incident to the boundary we require normal arcs α and β' contradicting the Torus Arc Lemma.

Case 3: Finally we must treat the case in which the branch pyramid has no normal quad

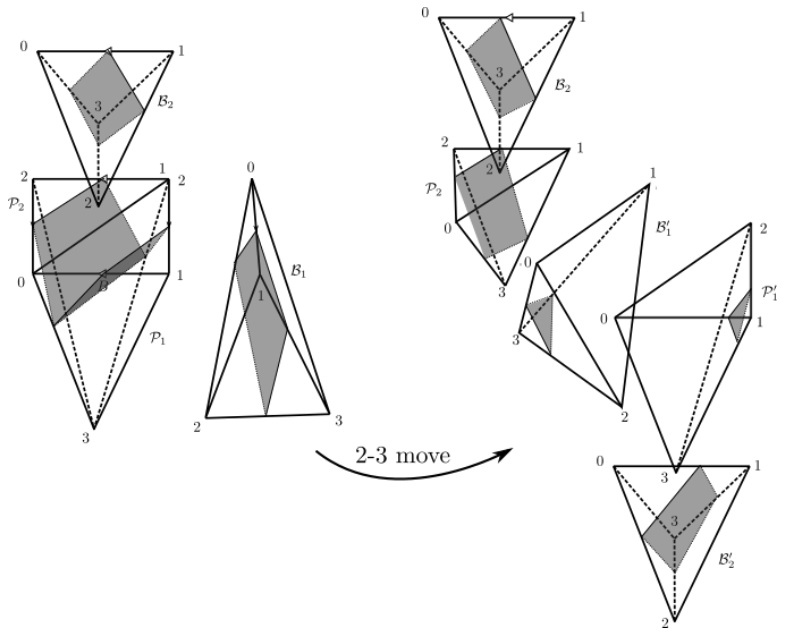

Figure 23: Arcs γ and γ' carrying normal quads and the 2-3 move to collect normal quads in band 2. The gluings after the 2-3 move are given in Table 15.

tet	(012)	(013)	(023)	(123)
$(\mathcal{P}_1')$		$(\mathcal{B}_2')(013)$	$(\mathcal{B}_1')(012)$	$(\mathcal{P}_2)(023)$
$(\mathcal{P}_2)$		$(\mathcal{B}_1')(013)$	$(\mathcal{P}_1')(123)$	$(\mathcal{B}_2)(102)$
$(\mathcal{B}_1')$	$(\mathcal{P}_1)(023)$	$(\mathcal{P}_2)(013)$	$(\mathcal{B}_2')(032)$	
$(\mathcal{B}_2)$	$(\mathcal{P}_2)(213)$	$(\mathcal{B}_2')(012)$		
$(\mathcal{B}_2')$	$(\mathcal{P}_1')(013)$	$(\mathcal{B}_2)(013)$		$(\mathcal{B}_1')(032)$

Table 15: Gluings after the 2-3 move in Figure 23

types present. By the Torus Arc Lemma, we must have either the arcs γ, γ' or the collection $\alpha, \beta', \alpha', \beta$. Both instances give admissible normal surface solutions and the process works exactly as illustrated in Figure 22. The appropriate 2-3 move collects all incompatible quads in a single band and after shortening we apply Corollary 4.3.1. Thus we complete the proof. ■

To summarize the observations found in the subcases of the previous proof, in a short inflation, only one pair of $(\alpha, \alpha'), (\beta, \beta'), (\gamma, \gamma')$ can carry normal quads for the surface S to

be a properly embedded normal surface. There is an alternate proof of Theorem 4.3.1 using the gluing equations coming from the subcomplex $\mathbf{\Delta}_\xi$ similiar to that found in the proof of Lemma 4.3.2. The cases in Theorem 4.3.1 are analogous to the various constraints placed by the Quadrilateral Condition. It is necessary to include condition that the boundary of M be homeomorphic to a torus as opposed to allowing Klein bottles. In particular Lemma 4.3.2 does not hold.

We now build upon Theorem 4.3.1 to produce an algorithm to build an ideal triangulation in which a fiber of a bundle structure spun-normalizes. This algorithm yields a bounded subset of the solution space of normal surfaces in which to find said spun-normal fiber.

Theorem 4.3.2 *Let K be a compact, irreducible, ∂-irreducible, atoroidal 3-manifold with nonempty, connected boundary a torus. Further suppose that K is an orientable S^1-bundle over an essential fiber F. There is an algorithm to build an ideal triangulation of the interior of K in which F spun-normalizes. The algorithm finds the spun-normal surface.*

Proof. Let K be a compact, irreducible, ∂-irreducible, atoroidal 3-manifold with nonempty, connected boundary a torus. By Theorem 2.3.1 (Lackenby) there is an algorithm to construct a taut ideal triangulation, $\mathcal{T}^*$, of K. Our algorithm takes as input this taut ideal triangulation, $\mathcal{T}^*$. By Proposition 2.3.1, $\mathcal{T}^*$ is 1-efficient. Suppose that $|\mathcal{T}^*| = n$. We can construct a frame ξ for $\mathcal{T}^*$. By Proposition 3.0.1 the inflation triangulation $\mathcal{T}_\xi$ is 0-efficient. By Theorem 2.3.3 (Schleimer) a fiber F for the bundle structure can be found amongst the fundamental surfaces of $\mathcal{T}_\xi$. If F is in C-position we are done by Lemma 4.2.1 (due to the correspondence of Q-coordinates). Suppose F is not in C-position, and let $\mu = ||\vec{F}_Q||$ be the number of normal quadrilaterals of F. By Theorem 4.3.1 and Remark 2.5.1 we can modify $\mathcal{T}_\xi$ to a short inflation triangulation $\mathcal{T}'_\xi$ in which $F' \cong F$ is in C-position with $\#(\text{2-3 moves}) \leq len(\xi) + 4 < 8n + 4$. While it is not necessary that $\mathcal{T}'_\xi$ be 0-efficient, we can find F' within the bounds $||\vec{F}'_Q|| < \mu + \mu(8n + 4) = \mu(8n + 5)$. Let $\mathcal{T}^C$ be the ideal triangulation obtained from $\mathcal{T}'_\xi$ by crushing ∂K. As F' is in C-position, F spun-normalizes in $\mathcal{T}^C$.

It follows the spun-normalization can be found within the same bounds $||\vec{F}_Q|| < \mu(8n+5)$ in $\mathcal{T}^C$. ■

Theorem 4.3.1 answers Cooper, Tillmann, and Worden affirmatively. The following theorems, extending Theorem 4.3.1 to manifolds with multiple torus boundary components, give partial answers to a question of Walsh. We note that Walsh poses the question of spun-normalizing fibers for a fixed ideal triangulation. We show that there is an ideal triangulation in which the fiber can be realized as a spun-normal surface.

Theorem 4.3.3 *Given a 3-manifold M with boundary each component of which is a torus. Let S be a properly embedded incompressible, ∂-incompressible surface in M with non empty boundary, such that for each component B_i of ∂M, $\partial S \cap B_i$ is a single curve which is not nullhomotopic in B_i. Then there exists an ideal triangulation of the interior of M in which S spun-normalizes.*

Proof. Suppose that M has n boundary components. Let $\{B_i\}_{i\leq n}$ be an ordering of the boundary components of M. Let $(\mathcal{T}^*, \Lambda)$ be a framed triangulation of M, each vertex of which is ideal. Let $\mathcal{T}_\Lambda$ be the inflation of $\mathcal{T}^*$ with respect to Λ. By Theorem 2.2.3 (Haken), S is realized as a normal surface S' in $\mathcal{T}_\Lambda$. Consider a component B_0 of ∂M, Σ_0 the boundary link of B_0. We have two cases.

Case 1: If S' is in C-position with respect to Σ_0, crush $\mathcal{T}_\Lambda$ along Σ_0 to the framed triangulation $(\mathcal{T}_0^*, \Lambda_0)$. There is then a spun-normal representative S_0 of S that spins around the cusp at the ideal vertex representing B_0 in $\mathcal{T}_0^*$.

Case 2: If S' is not in C-position with respect to Σ_0, crush $\mathcal{T}_\Lambda$ to $\mathcal{T}'_\Lambda$ at all boundary components other than B_0. By Proposition 4.1.1 we can shorten $\mathcal{T}'_\Lambda$ to a short inflation at B_0. Applying the techniques of Theorem 4.3.1, we can arrive at an inflation triangulation in which F is in C-position with respect to B_0. Crush $\mathcal{T}'_\Lambda$ along the normalization of a pushoff of B_0. Inflate all boundary components other than B_0, call this the framed triangulation $(\mathcal{T}_0^*, \Lambda_0)$. Again there is a spun-normal representative S_0 of S that spins around the cusp at

the ideal vertex represent B_0 in $\mathcal{T}_0^*$.

Notice in the above cases, $\mathcal{T}_0^*$ has only one ideal vertex. Iterating this process over each boundary component B_i, if S_{i-1} is in C-position with respect to Σ_i, crush $\mathcal{T}_{i-1}^*$ along Σ_i. Otherwise crush all boundary components other than B_i to $(\mathcal{T}_{i-1}^*)'$. As in Case 2 we can shorten $(\mathcal{T}_{i-1}^*)'$ to a short inflation at B_i. We can again arrive at an inflation triangulation in which S_{i-1} is in C-position with respect to B_i. Crush $(\mathcal{T}_{i-1}^*)'$ along the normalization of B_i and inflate all boundary components B_j with $j > i$. Call the resulting framed triangulation $(\mathcal{T}_i^*, \Lambda_i)$. There is a spun-normal representative S_i of S that spins around the cusp at the ideal vertex representing B_i in $\mathcal{T}_i^*$. By Remark 4.1.1 S_i also spins around each cusp at the ideal vertices representing $\{B_j\}$ for $j < i$.

Finally we have the ideal triangulation $\mathcal{T}_n^*$ in which S is realized as the spun-normal surface S_n, completing the proof. ■

We now present an extension to Theorem 4.3.3, analogous to Theorem 4.3.2, giving an algorithm to build an ideal triangulation for a 3-manifold with multiple torus boundary components in which a fiber of a bundle structure spun-normalizes. As with in Theorem 4.3.2, the algorithm finds the spun-normal surface amongst the solutions to the Q-matching equations.

Theorem 4.3.4 *Let L be a compact, irreducible, ∂-irreducible, atoroidal 3-manifold with nonempty boundary, each component of which is a torus. Further suppose that L is an orientable S^1-bundle over an essential fiber F. There is an algorithm to build an ideal triangulation of the interior of L in which F spun-normalizes. The algorithm finds the spun-normal surface.*

Proof. Let L be a compact, irreducible, ∂-irreducible, atoroidal 3-manifold with nonempty boundary, each component of which is a torus. The algorithm takes as input an ideal triangulation, $\mathcal{T}^*$, of the interior of L. Suppose that $|\mathcal{T}^*| = n$. We can construct a framing Λ for $\mathcal{T}^*$. By Theorem 2.2.3 (Haken) a fiber F for the bundle structure must be amongst

the normal surfaces of $\mathcal{T}_\Lambda$. We can find F by enumerating the fundamental surfaces of $\mathcal{T}_\Lambda$. If F is not found amongst the fundamental surfaces, we take finite linear combinations of non-negative integral multiples of fundamental surfaces until F is identified. If F is in C-position, by Lemma 4.2.1 (due to the correspondence of Q-coordinates), we are done. Suppose F is not in C-position, and let $\mu = ||\vec{F}_Q||$ be the number of normal quadrilaterals of F. By Theorem 4.3.3 and Remark 2.5.1, we can modify $\mathcal{T}_\Lambda$ to a short inflation triangulation $\mathcal{T}'_\Lambda$ in which $F' \cong F$ is in C-position with $\#(\text{2-3 moves}) \leq len(\Lambda) + 4m < 8n + 4m$, where m is the number of boundary components of L. We can find F' within the bounds $||\vec{F}'_Q|| < \mu + \mu(8n + 4m) = \mu(8n + 4m + 1)$. Let $\mathcal{T}^C$ be the ideal triangulation obtained from $\mathcal{T}'_\Lambda$ by crushing ∂L, and F^C the image of F' under the crushing map. As F' is in C-position, F^C spun-normalizes in $\mathcal{T}^C$. ■

As F' can be found within the bounds $||\vec{F}'_Q|| < \mu+\mu(8n+4m) = \mu(8n+4m+1)$, it follows that the spun-normalization can be found within the same bounds $||\vec{F}_Q|| < \mu(8n+4m+1)$ in $\mathcal{T}^C$. It was important in the proof of Theorem 4.3.3 to crush all boundary components other than the one being shortened. This is due to the potential of crossings at branch points. Proposition 4.1.1 does not handle such cases.

Theorem 2.3.1 due to Lackenby [13] has an associated algorithm that begins with a *taut sutured manifold hierarchy* [13] on L (or K) and constructs a taut ideal triangulation. Our algorithms in both Theorems 4.3.2 and 4.3.4 can take as input this taut ideal triangulation. This appears as a natural starting position for our use. However, one can start with any 1-efficient ideal triangulation. We also point out that our final ideal triangulation $\mathcal{T}^C$ is not necessarily 1-efficient. Hence, recent results of Kang and Rubinstein [11] relating to spun-normalization of fibers are not applicable here. Further, our methods produce an ideal triangulation in which a surface spun-normalizes. The work of Kang and Rubinstein produces spun-normal surfaces given conditions on a triangulation.

The primary difference between the algorithms found in Theorems 4.3.2 and 4.3.4, is the use of Theorem 2.3.3 (Schleimer). Because we can identify the fiber amongst the fundamental

surfaces when K has one torus boundary component, starting from a 1-efficient ideal triangulation we are able to build $\mathcal{T}^C$ and identify the spun-normalization of F in bounded time. In contrast, we currently can only say the fiber exists as a normal surface in the triangulation $\mathcal{T}_\Lambda$, and can give no bounds on the time it takes to find this normal representative. That is, the algorithm presented in Theorem 4.3.4 comes with no time complexity bounds. We do still include efficiency in the proof of Theorem 4.3.4, as this seems the natural requirement leading to the identification of F^C in the shortest time.

REFERENCES

[1] Steve Armentrout, *Cellular decompositions of 3-manifolds that yield 3-manifolds*, Bulletin of the American Mathematical Society **75** (1969), no. 2, 453 – 456.

[2] Birch Bryant, William Jaco, and J. Hyam Rubinstein, *Efficient triangulations and boundary slopes*, Topology and its Applications **297** (2021), 107689.

[3] Benjamin A. Burton, *The Pachner graph and the simplification of 3-sphere triangulations*, Proceedings of the twenty-seventh annual symposium on Computational geometry, ACM, jun 2011.

[4] Benjamin A. Burton, Ryan Budney, William Pettersson, et al., *Regina: Software for low-dimensional topology*, `http://regina-normal.github.io/`, 1999–2021, ver. 5.1.

[5] Daryl Cooper, Stephan Tillmann, and William Worden, *The Thurston norm via spun-normal immersions*, 2021, In preparation.

[6] David Futer, Emily Hamilton, and Neil R. Hoffman, *Infinitely many virtual geometric triangulations*, Journal of Topology **15** (2022), no. 4, 2352–2388.

[7] William Jaco and Hyam Rubinstein, *Inflations of ideal triangulations*, Advances in Mathematics **267** (2013), 176–224.

[8] William Jaco and J. Hyam Rubinstein, *0-efficient triangulations of 3-manifolds*, Journal of Differential Geometry **65** (2002), 61–168.

[9] William H. Jaco and J. Hyam Rubinstein, *Layered-triangulations of 3-manifolds*, 2006.

[10] Ensil Kang and J Hyam Rubinstein, *Ideal triangulations of 3-manifolds II taut and angle structures*, Algebraic & Geometric Topology **5** (2005), no. 4, 1505–1533.

[11] ———, *Spun normal surfaces in 3-manifolds, I: 1-efficient triangulations*, Algebraic & Geometric Topology **22** (2022), no. 8, 3533–3576.

[12] Hellmuth Kneser, *Geschlossene flächen in dreidimensionalen mannigfaltigkeiten.*, Jahresbericht der Deutschen Mathematiker-Vereinigung **38** (1929), 248–259.

[13] Marc Lackenby, *Taut ideal triangulations of 3–manifolds*, Geometry & Topology **4** (2000), no. 1, 369–395.

[14] Saul Schleimer, *Almost normal Heegaard splittings*, Doctoral Thesis, University of Berkeley (1994).

[15] L.C. Siebenmann, *Approximating cellular maps by homeomorphisms*, Topology **11** (1972), no. 3, 271–294.

[16] Jeffrey L. Tollefson, *Normal surface Q-theory*, Pacific Journal of Mathematics **183** (1998), 359–374.

[17] W. v. Haken, *Über das homöomorphieproblem der 3-mannigfaltigkeiten. i*, Mathematische Zeitschrift **80** (1961), 89–120.

[18] Genevieve S. Walsh, *Incompressible surfaces and spunnormal form*, Geometriae Dedicata **151** (2011), 221–231.

VITA

Birch Bryant

Candidate for the Degree of

Doctor of Philosophy

Dissertation: FIBERS AS NORMAL AND SPUN-NORMAL SURFACES IN LINK MANIFOLDS

Major Field: Mathematics

Biographical:

Education:

Completed the requirements for the Doctor of Philosophy in Mathematics at Oklahoma State University, Stillwater, Oklahoma in May, 2023.

Completed the requirements for the Bachelor of Science in Mathematics at Southeastern Oklahoma State University, Durant, Oklahoma in 2016.

Professional Memberships:

American Mathematical Society